MAY 2010

SAN FRANCISCO ESTUARY & WATERSHED SCIENCE
Sponsored by the Delta Science Program and the UC Davis John Muir Institute of the Environment

Mercury-Contaminated Hydraulic Mining Debris in San Francisco Bay

Robin M. Bouse, Christopher C. Fuller[1], Samuel N. Luoma[2], Michelle I. Hornberger, Bruce E. Jaffe, and Richard E. Smith
U.S. Geological Survey, 345 Middlefield Road, Menlo Park, CA 94025

ABSTRACT

The hydraulic gold-mining process used during the Californhttia Gold Rush and in many developing countries today contributes enormous amounts of sediment to rivers and streams. Commonly, accompanying this sediment are contaminants such as elemental mercury and cyanide used in the gold extraction process. We show that some of the mercury-contaminated sediment created by hydraulic gold mining in the Sierra Nevada, between 1852 and 1884, ended up over 250 kilometers (km) away in San Francisco Bay; an example of the far-reaching extent of contamination from such activities.

A combination of radionuclide dating, bathymetric reconstruction, and geochemical tracers were used to distinguish the hydraulic mining sediment from sediment deposited in the bay before hydraulic mining started (pre-Gold Rush sediment) and sediment deposited after hydraulic mining stopped (modern sediment). Three San Francisco Bay cores were studied as well as source material from the abandoned hydraulic gold mines and river sediment between the mines and bay. Isotopic and geochemical compositions of the core sediments show a geochemical shift in sediment deposited during the time of hydraulic mining. The geochemical shift is characterized by a decrease in εNd, total organic carbon (TOC), Sr and Ca concentrations, Ca/Sr, and Ni/Zr; and, an increase in $^{87}Sr/^{86}Sr$, Al/Ca, Hg concentrations, and quartz/plagioclase. This shift is in the direction of the geochemical signature of sediments from rivers and gold mines in hydraulic mining areas. Mixing calculations using Nd isotopes and concentrations estimate that the hydraulic mining debris comprises up to 56% of the sediment in core sediments deposited during the time of hydraulic mining. The surface sediment of cores taken in 1990 were found to contain up to 43% hydraulic mining debris, reflecting a continuing remobilization and redistribution of the debris within the bay and transport from the watershed.

Mercury concentrations in pre-Gold Rush sediment range between 0.03 and 0.08 μg g^{-1}. In core sediments that have characteristics of the gold deposits and were deposited during the time of hydraulic mining, mercury concentrations can be up to 0.45 μg g^{-1}. Modern sediment (post-1952 deposition) contains mercury concentrations up to 0.79 μg g^{-1} and is likely a mix of hydraulic mining mercury and mercury introduced from other sources.

1 Corresponding author: ccfuller@usgs.gov
2 Present address: John Muir Institute of the Environment, University of California at Davis, Davis, CA 95616

KEYWORDS

Sediment sources, neodymium, strontium, isotopes, mercury, mine tailings, USA, California, San Francisco Bay.

INTRODUCTION

When human activities add inorganic mercury to the environment, the most important environmental outcome is generation of methylmercury. This occurs when bacteria transfer a methyl group (CH_3) from an organic compound into a chemical bond with inorganic mercury (Morel and others 1998) via a complex series of reactions (Marvin-Depasquale and others 2000). Methylmercury (MeHg) is a potent neurotoxin and reproductive toxin. It is biomagnified through aquatic food webs, placing at risk people who consume predatory fish or for whom fish is a mainstay in their diet (Mergler and others 1998). Methylmercury also is an ecological hazard to fish and birds, in particular threatening charismatic predators, especially fish-eating wildlife (Heinz and Hoffman 1998; Wiener and others 2007).

Human sources of mercury input into the environment include energy production, mining and other types of industry (Luoma and Rainbow 2008). Throughout the world, tailings from hydraulic gold mining are of particular concern. In hydraulic mining, including artisan gold mining, traditional amalgamation methods are used to remove gold from ores. The ore is washed over a bed of mercury; the silver and gold amalgamate or attach to the mercury; then the Hg is volatilized and precious metals captured. About 25% to 50% the elemental mercury used to extract the gold remains with the sediments or is otherwise lost to the environment when large volumes of tailings are discharged to a watershed (Nriagu 1994). In oxidizing conditions this elemental mercury (Hg) can be converted to Hg^{+2} and ultimately some fraction will be methylated and biomagnify through the aquatic food web. Primitive gold mining remains an important activity in many parts of the developing world, from the Philippines to Brazil. It is thought that as many as 550,000 to 1,000,000 artisan miners were active in Latin America in the late 1990s (Malm 1998). Tracking the fate of the sediments originating from hydraulic mining, as well as the mercury that accompanies those sediments is thus a problem of global interest.

One way to determine the extent of this problem would be to identify deposits of hydraulic mining debris relative to other sediments, but that can be problematic. Dating methods for deposited sediments are often insufficient to precisely link dates of deposition to occurrence of hydraulic mining. The differences between the sediments from different sources also can be subtle, particularly after they are transported downstream from their source and mixed with other sediments. In this paper we define a geochemical signature unique to hydraulic mining debris in sediments of San Francisco Bay employing geochemical characteristics and isotopic tracers unique to ores typical of gold mining. We validate the signature using a relationship between the geochemistry of in-place sediments and the predicted location of hydraulic mining debris given by a historical bathymetry model. We then estimate the amount of mercury deposited in bay sediments associated with the hydraulic mining debris. To characterize the mining signature, sediment samples were taken from abandoned hydraulic gold mines in the Sierra-Nevada, from rivers draining from these mines to the bay, and from sediment cores in the bay itself that were dated using radionuclide profiles (Fuller and others 1999) and changes in bathymetry between 1856 to 1983 (Jaffe and others 1998).

Mercury and Hydraulic Mining in the San Francisco Bay and Sacramento-San Joaquin Delta

Mercury contamination is of particular concern to the San Francisco Bay and Sacramento-San Joaquin Delta, partly because the geology of the area supports mercury mining and partly because hydraulic mining, was the dominant type of mining in the Sierra Nevada during the latter stages of the California Gold Rush (James 2005). There is some evidence that the combination of intense mercury mining and widespread mobilization of sediments during the hydraulic mining era dispersed mercury across the watershed. Elevated mercury concentrations are found in the delta and the bay in water and sedi-

ments (Domagalski 2001; Heim and others 2007), as well as biota from throughout the food web, including sport fish (Davis and others 2002, 2008). Cores of dated sediments from San Francisco Bay show that increases in mercury concentrations began to exceed pre-anthropogenic levels of ~0.07 µg g^{-1} dry weight about the time of the hydraulic mining era (Hornberger and others 1999). However, the exact fate and distribution of these sediments and their accompanying contamination are not well known (Conaway and others 2008) because no methodologies were available to identify the hydraulic mining debris.

In the Sierra Nevada, gold mining and the associated use of elemental mercury began with the 1849 Gold Rush and continued for over 30 years. Gold panning in Sierra Nevadan streams was replaced by the hydraulic gold-mining technique in 1852. Hydraulic mining was wide spread until 1884 when it was halted by a court order. During hydraulic gold mining large pressurized water cannons are aimed at hillsides of unconsolidated gold-rich gravels. The gravels are washed into an extensive series of sluices to which mercury is added. Mercury and gold form an amalgam that collects in the bottom of the sluices. The amalgam is collected; mercury is roasted away from the amalgam; and gold remains. Although this type of mining and refining is now obsolete in North America, unregulated mining practices still persist in developing countries (Meech and others 1998; Jacobson and Kratochvil 1998).

Mercury used for gold mining in the Sierra Nevada was mined in the Coast Range as cinnabar and refined to elemental mercury (Figure 1A). Approximately 60,000 tonnes of mercury was produced between 1850 and 1900 and used in gold mining mainly along the Yuba, Bear, and American rivers (Nriagu 1994; James 2005) (Figure 1A). Historical accounts suggest that 25% to 30% of the mercury can be lost in mine tailings and wastewater (Nriagu 1994), although in some cases it is estimated that as much as 50% of the mercury has been lost to the environment (Meech and others 1998).

Between 1856 and 1887, over 400 million cubic meters (m^3) of sediment were deposited in San

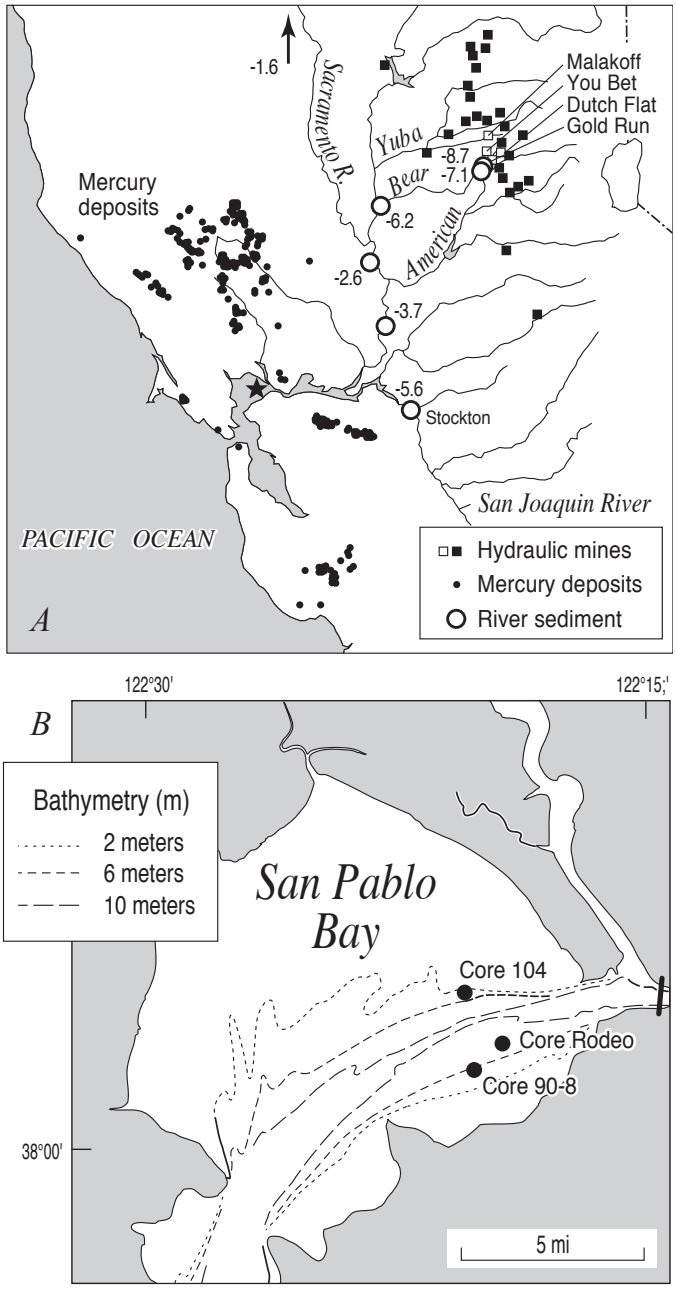

Figure 1 **(A)** Location of mercury mines in the Coast Range and hydraulic gold mines in the Sierra Nevada. The four hydraulic gold mines sampled in this paper are shown as open squares (Malakoff Diggins, Dutch Flat, Gold Run, and You Bet). The open circles are the locations of river sediment and their corresponding εNd value. The star is the location of Figure 1B. **(B)** Location of the three sediment cores recovered in San Pablo Bay.

Francisco Bay as a result of the hydraulic mining operations (Jaffe and others 1998). The sedimentation rate in San Pablo Bay during this time increased dramatically. The areal extent of the delta increased and reliable ship navigation was affected (Gilbert 1917). This large sediment volume counteracted shoreline retreat caused by rising sea level and built many marshes and islands in the bay-delta system (Gilbert 1917; Peterson and others 1993; Jaffe and others 1998). Many of those wetlands were eventually developed for human use and some are now undergoing, or being proposed for, reconversion to wetlands (for example, Davis and others 2003). Wetland sediments generate methylmercury faster than shallow water sediments throughout the world (Krabbenhoeft and others 1999) and in San Francisco Bay (Marvin-Depasquale and others 2000). Therefore there is a concern that wetlands restoration could accelerate mercury contamination of the bay ecosystem (Davis and others 2003). A protocol to determine how much hydraulic mining debris might occur in specific wetlands could therefore be quite valuable.

METHODS

Field Sites and Sample Collection

The dominantly quartz-rich gravels that bear gold have a distinct lithology from other rock units in the watershed (James 1991a), which could offer opportunities to identify and geochemically characterize hydraulic mine tailings. Neodymium (Nd) isotopes are of interest, in particular, because sediments retain the Nd isotopic signature of their source throughout weathering, transport, deposition, and diagenesis (Faure 1986). Strontium (Sr) isotopes and major and trace element studies are also useful tools in determining sediment source regions but can under go some alteration during the weathering process (Ingram and Sloan 1992). For example, interaction with seawater can alter the Sr isotopic composition of sediments while the Nd isotopic composition remains relatively unchanged partly because the Sr concentration in seawater is 8 mg L^{-1} but the Nd concentration is only 2.6 x 10^{-6} mg L^{-1} (Faure 1986).

The auriferous (gold-bearing) gravels that were hydraulically mined in the Sierra Nevada were laid down by Eocene streams about 50 million years ago (Lindgren 1911; Yeend 1974). The stream channels cut into the underlying Paleozoic and Mesozoic metasedimentary and metavolcanic rocks that were intruded by Late Jurassic and Cretaceous Sierra Nevadan batholiths (Schweickert 1981). The clasts in the Eocene gravels are predominantly quartz. Next in abundance are clasts of slate and phyllite. Less abundant clasts are igneous rocks, predominantly granodiorite. The auriferous gravels can be divided into upper and lower gravel strata based on lithology and texture, although the contact between them is gradational and does not apply to every location (Yeend 1974). The lower gravels contain cobble and boulder size clasts of underlying bedrock (mainly slates and phyllites) whereas pebble size and smaller clasts (mostly quartz) predominate in the upper gravels. Miners sought the lower gravel because gold is heavy and often trapped in the stream channel crevices. The lower gravels are often cemented with silica and could not be hydraulically mined so they were mined by tunneling along the gravel-bedrock contact. The upper gravels, also rich in gold, are unconsolidated, interstratified with beds of sand, silt and clay, and locally stained to various hues of orange (10YR 8/2, 10YR 8/6, 10YR 7/4 and 10YR 6/6), particularly in the uppermost soil horizons. The beds overlying the upper gravel consist mainly of bentonite, tuff, and andesite breccia. The upper gravel is differentiated from the overlying units by its lack of fresh volcanic material (Yeend 1974).

Samples of the upper gravels were collected from four of the largest, richest, and most extensively mined deposits of the auriferous gravels. They are located in the Colfax quadrangle (Lindgren 1911), and include the North Bloomfield (Malakoff Diggins), Dutch Flat, You Bet, and Gold Run mines (Figure 1A). The purpose was to represent the range of source material that was transported downstream as a result of hydraulic mining. Sediments remaining in the hydraulic mines were sampled from trenches that cut approximately 0.1 meters (m) horizontally and 30 m vertically down cliff faces perpendicular to bedding. Surface material on the cliff face was avoided. Generally 10-m sections were aggregated into one sample. The sediments were collected on large plas-

tic sheets at the base of the cliff. Clasts greater than pebble size were removed. Approximately 0.25 m^3 of sediment was collected. This material was then wet sieved to <63 µm with deionized water and nylon mesh.

Bed sediments from streams and rivers were collected because they are good integrators of the isotopic compositions of rocks in the area. Bed sediment was collected from two streams in the hydraulic mining area, several locations in the Sacramento River, and one location in the San Joaquin River. The bed sediment was collected from depositional point bars.

Cores analyzed in this study were collected at three different sites in San Francisco Bay (Figure 1B). Two cores (Core 90-8 and Rodeo) were collected from southeastern San Pablo Bay, south of the main ship channel. Core 104 is from the north side of the channel. The Rodeo Core location is closer to the main channel than Core 90-8. Cores 90-8 and 104 are USGS gravity cores (9-cm inner diameter), 2.4 m and 1.9 m in length, respectively, collected in 1990. The Rodeo Core is a piston core (10-cm inner diameter) that extends 6.7 m in length, collected in 1993 (Ingram and others 1996). The core liners were extracted from their barrels, capped, sealed, and transported upright to cold storage (2-3°C). The cores were X-rayed, split, and subsampled for geochemical analyses (Ingram and others 1996; Hornberger and others 1999). Both Cores 90-8 and Rodeo have been previously studied. Radioisotopic dating along with inorganic and organic contaminant measurements were used to evaluate the historical inputs of contaminants to San Francisco Bay (van Geen and Luoma 1999, and papers therein). Bivalve shells in the Rodeo core were carbon-14 (^{14}C) dated and analyzed for Sr isotopes to determine inflow into the bay from the Sacramento and San Joaquin rivers (Ingram and others 1996).

Analytical Methods

All geochemical analyses were preformed on the <63-µm fraction of sediment to minimize grain size bias (Hornberger and others 1999) and to capture sediment most easily transported to the San Francisco Bay. Approximately one-gram subsamples of core material were wet sieved through 63-µm mesh-screen into 100-ml beakers and dried. Each dried <63-µm sample was homogenized with a mortar and pestle and subsampled. The subsamples were weighed, dried again in a 70° oven, cooled in a desiccator and reweighed for geochemical analyses. The >63-µm fractions were air dried in previously weighed Petri dishes, then weighed. Total organic carbon (TOC) was determined by finding the difference between total carbon and carbonate using a total combustion carbon LECO analyzer.

For isotopic and elemental analyses, 100 mg of <63-µm sediment was digested in a series of concentrated HF, HNO_3 and 6N HCl dissolutions following the method described in Marvin-DiPasquale and others (2003). Upon complete dissolution, a 20% portion of each sample was taken for bulk chemical analyses. This portion was dried, then reconstituted in 50 ml of 2% HNO_3 plus 0.2 ml of internal standard, which was added for elemental analyses on an inductively coupled plasma mass spectrometer (ICPMS). The analytical errors for all elements presented in this study were less than ±5%.

The remaining 80% of each sample was put through a series of ion exchange columns to separate Sr and Nd as described by Bullen and others (1997) and Marvin-DiPasquale and others (2003), respectively. The Sr and Nd fractions were dried down with HNO_3, H_3PO_4, and H_2O_2. Sr and Nd isotopic ratios were measured by thermal ionization mass spectrometry (TIMS) with the resulting Sr and Nd ratios normalized to correct for mass fractionation using $^{86}Sr/^{87}Sr$ = 0.1194 and $^{143}Nd/^{144}Nd$ = 0.7219 (Bullen and Clynne 1990). The maximum uncertainty for $^{87}Sr/^{86}Sr$ is ±0.00003 and for $^{143}Nd/^{144}Nd$ ±0.00002. $^{143}Nd/^{144}Nd$ was converted to εNd using the value 0.512636 for CHUR (condritic uniform reservoir).

Quartz content relative to plagioclase was determined by X-ray diffraction. The X-ray diffraction patterns were obtained on a Philips X-ray diffractometer with carbon monochromator and Cu K_α radiation. Continuous scans were run from 4-70° 2θ at 40 kV and 45 mA. The quartz/plagioclase ratio was calculated using the area under the major quartz peak at 26.6° 2θ divided by the area under the major plagioclase peak at 28.0° 2θ.

An experiment to determine Sr exchange was conducted on four unwashed bay sediment samples and sediment from one hydraulic mine following the method described by Bullen and others (1997). Approximately 2.5 g of <63-µm sediment and 50 ml of ammonium acetate were shaken in 60-ml bottles for 24 h. The bottles were removed from the shaker and the sediment settled for 48 h. The supernatant was filtered through a 0.45 µm filter. A 2-ml aliquot was taken from the supernatant and analyzed by ICPMS for elemental concentrations. Approximately 20 ml of the supernatant was dried, taken up in 2 ml of 2N HCl, and put through cation exchange columns to separate Sr for isotopic analyses by TIMS. The remaining residue sample was filtered, washed, and dried. A 100-mg sample of this residue was digested, split, eluted, and analyzed by ICPMS and TIMS in the same manner described above for sediment samples.

Total mercury in the <63-µm sediment samples were determined following the method of Elrick and Horowitz (1986). The samples were reacted with aqua regia at 100°C and reconstituted with 10% nitric dichromate. Before analyses, 3% $NaBH_4$ (in 1% NaOH) was added as a reductant. The total Hg analyses were conducted by cold vapor atomic absorption spectroscopy. The method detection limit is 0.01 µg g^{-1} and precision ±10% for concentrations greater than 0.1 µg g^{-1}. No significant loss of Hg was found during sample drying at temperatures to 105°C when compared to drying at room temperature (Elrick and Horowitz 1986).

Dating Techniques

The cores were dated using the radionuclides ^{137}Cs, $^{239,240}Pu$, and ^{210}Pb (Fuller and others 1999). The fallout radionuclides ^{137}Cs and $^{239,240}Pu$, introduced into the environment by atomic weapons testing between 1952 and 1964, are only detected in horizons containing a component of sediment deposited after 1952 (Figure 2). The detection limit for the low abundances of excess ^{210}Pb in bay sediments limits this dating technique to ~60 years (Fuller and others 1999). Thus, for San Francisco Bay, radionuclide dating cannot define sediment deposited during the time of hydraulic mining.

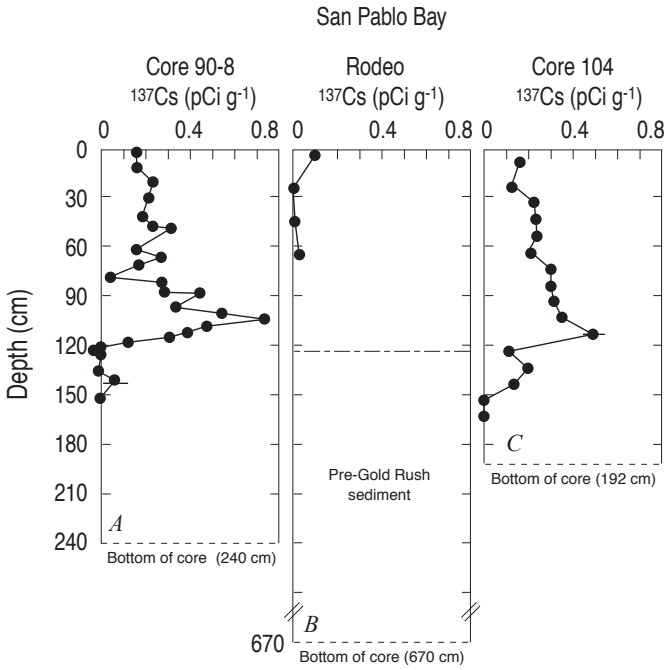

Figure 2 ^{137}Cs activity in picoCuries per gram (pCi g^{-1}) versus depth in the three San Pablo Bay cores. Dashed line in Rodeo core profile indicates depth horizon of onset of hydraulic mining.

Higgins and others (2005) devised a novel approach for estimating the location of sediment deposited during the hydraulic mining period in San Francisco Bay. Data from bathymetric surveys conducted about every 20 to 30 years since 1856 were reconstructed on a 100-m grid. Depth soundings were corrected for tides, and a 50-m bathymetric grid was developed for each time slice. The grids were brought to a common vertical datum by removing sea level change and a sedimentation history was determined for each of the three core locations (Figure 3). Comparisons of sediment surfaces for survey dates were then used to estimate depth changes attributable to sediment deposition or erosion. These bathymetric reconstructions from six surveys (1856, 1887, 1898, 1922, 1951, 1983) reveal dynamic changes in bay floor topography through time and space. The sedimentation from 1983 to the date of core collection was extrapolated using the 1951 to 1983 rate for each core. The historical bathymetry model ages for sediment horizons compared well with radioisotopic dating of sediment cores (Higgins and others 2007). Results from the historical bathymetric model were used to estimate that

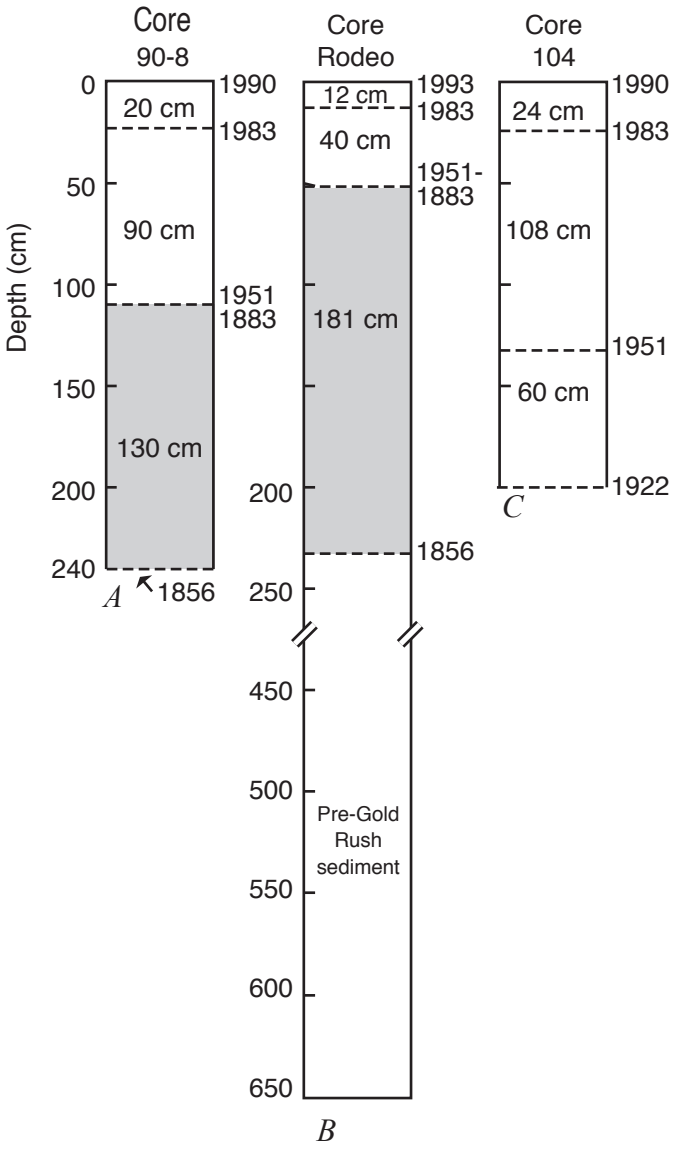

Figure 3 Historical bathymetry reconstructions of net sediment deposition at each core location. Dashed lines represent the dates 1856, 1883, 1922, 1951, and 1983 predicted by the historical bathymetry model (Higgins and others 2005). Cores 90-8 and 104 were collected in 1990 and Core Rodeo in 1993; these dates are at the top of the core. Gray shading indicates the period of hydraulic mining.

a large volume of sediment (400,000,000 m^3) was deposited between 1856 and 1887 that may be attributed to hydraulic mining. Geochemical analyses presented here are used in part to validate this finding.

Several geochemical properties were used as indicators of the hydraulic mining period. Sediments deposited since the Gold Rush are characterized by trace element enrichment due to human activities, with the greatest enrichment for the most elements occurring after the turn of the century. These enrichments can be used to generally characterize sediments deposited in the last 50 to 150 years (Hornberger and others 1999). Large increases in Pb concentrations with less radiogenic Pb isotopic compositions occur in the core sediments deposited after ~1880 (Ritson and others 1999).

Carbon-14 ages of shells were used to date sediment deposited before the Gold Rush (Ingram and others 1996). In addition, the first appearance of certain bivalve species help bound the age of more recent sediment. Non-native species have been transported to San Francisco Bay at various times since the Gold Rush of 1849. An example is *Mya areneria*, the eastern soft shell clam, that was introduced in to the bay sometime between 1869 and 1874 (Conomos 1979; Nichols and others 1986).

RESULTS AND DISCUSSION

Geochemical Characteristics of Source Materials: Hydraulic Mine and River Sediments

The geochemical characterization of sediments from the hydraulic mine sites and streams draining these areas provide end members to which the San Francisco Bay core sediment can be compared. The analyses show that the chemistry of the hydraulic mine gravels is relatively similar among the mines (Table 1). The deposits all have a high chemical index of alteration (CIA > 90), where CIA = Al_2O_3/(Al_2O_3+CaO+Na_2O+K_2O) *100 (Nesbitt and Young 1982; Taylor and McLennan 1985). This weathering index measures the degree of alteration of feldspar to clay. A CIA greater than 90 indicates that most of the alkali and alkaline earth elements have been lost through extensive weathering. By comparison, the average CIA for shale is 70 to 75. In particular, Al/Ca in the hydraulic mines is much higher than in the Sacramento River bed sediment and background core sediment in the bay. It would be expected that

Table 1 Geochemistry and isotopic ratios of sediment from hydraulic gold mines

	You Bet Pit upper cliff face in mine	Highway 80 roadcut east of Gold Run exit	Highway 80 roadcut east of Gold Run exit	Gold Run upper cliff face above monitor	Gold Run lower cliff face near monitor	Dutch Flat middle cliff face in mine area	Malakoff upper cliff face mine west side	Malakoff lower cliff face mine west side
Al_2O_3 (μg g^{-1})	213,101	>150,000	>150,000	>150,000	>150,000	>150,000	128,211	195,373
K_2O (μg g^{-1})	18,145	16,887	14,324	11,740	11,366	11,822	12,178	12,078
NaO (μg g^{-1})	895	623	709	277	477	1337	432	456
CaO (μg g^{-1})	468	546	505	162	249	298	167	384
CIA	92	>90	>90	>90	>90	>90	91	94
Fe (%)	4.1	3.5	3.1	6.0	2.9	5.2	1.8	1.6
Nd (μg g^{-1})	20.0	23.2	21.6	17.7	17.0	18.8	17.2	25.3
Ni (μg g^{-1})	16	14	20	11	12	36	28	17
Pb (μg g^{-1})	14.8	14.8	10.4	20.9	15.2	15.5	10.0	7.9
Sr (μg g^{-1})	88	65	39	18	23	39	13	15
Zr (μg g^{-1})	134	96	104	91	60	104	86	116
Al/Ca	337	>200	>200	>200	>200	>200	568	377
Zr/Hf	37	34	33	36	36	36	35	38
Ca/Sr	4	6	9	6	8	5	9	18
Ni/Zr	0.1	0.1	0.2	0.1	0.2	0.3	0.3	0.1
εNd	-5.6	-5.7	-5.9	-6.9	-8.0	-8.7	-12.0	-13.9
$^{144}Nd/^{143}Nd$	0.512348 (10)	0.512344 (28)	0.512336 (16)	0.512281 (14)	0.512224 (11)	0.512138 (10)	0.512021 (16)	0.511925 (20)
$^{87}Sr/^{86}Sr$	0.71087 (2)	0.71147 (1)	0.71092 (1)	0.71318 (1)	0.71804 (1)	0.72551 (1)	0.74330 (1)	0.74553 (4)

a large influx of sediment from hydraulic mines into the bay would raise the Al/Ca of bay sediment.

Although the elemental concentrations are similar among the hydraulic mines, there is a wider range of isotopic values, for example: εNd = -5.6 to -13.9 and $^{87}Sr/^{86}Sr$ = 0.711 to 0.746 (Table 1). The least negative εNd sample also has the highest potassium concentration and comes from the top of You Bet Pit. This sample is likely representative of the upper most gravels and some of the volcanic overburden that was removed by the hydraulic mining. The gravels along Highway 80 at Gold Run have similar εNd and $^{87}Sr/^{86}Sr$ to those in upper You Bet Pit. The εNd at the base of the You Bet Mine is more negative and was taken from the bank of Steephollow Creek below the mine (Table 1). The most negative εNd is a sample from the Malakoff Diggins that has the highest Nd concentration and the lowest Sr and Pb concentrations.

There is a progression to less negative εNd downstream from the hydraulic mining areas to sediments in the Sacramento River. The εNd values from the bed sediment of two streams in the hydraulic mine area are Steephollow Creek at -8.74, and three miles downstream, Greenhorn Creek at -7.10; (Figure 1; Tables 1 and 3). Fifty kilometers downstream, the εNd of Bear River sediment at Wheatland is -6.14 while Sacramento River bed sediment below Bear is –2.6 (Table 3). A progression is also found in $^{87}Sr/^{86}Sr$: 0.71174, 0.70967, 0.70692, and 0.70603, respectively. In comparison, bed sediment transported toward the bay from the south via the San Joaquin River near the town of Stockton has εNd of -5.6 and $^{87}Sr/^{86}Sr$ of 0.7072 (Figure 1).

The isotopic compositions of hydraulic mine sediments are significantly higher in $^{87}Sr/^{86}Sr$ and more negative in εNd than the Sacramento River bed sediment. Bed sediment in the north Sacramento River (near Lake Shasta) has εNd of -1.6. Below the confluences of the Yuba and Bear rivers, Sacramento River bed sediment (near Verona) has εNd of -2.6 and $^{87}Sr/^{86}Sr$ of 0.70603. Below the confluence of the American River (near Hood), εNd decreases to

-3.7 and $^{87}Sr/^{86}Sr$ increases to 0.70629 (Figure 1). It appears that sediment released from the hydraulic mining areas may have increased the $^{87}Sr/^{86}Sr$ and decreased the εNd of bed sediment in the rivers, but their effect is diluted by background sediment from non-mined areas as the sediment is transported toward the bay (Figure 1).

Core Descriptions and Age Constraints

The depositional environment of San Francisco Bay is complex; areas of erosion, deposition, and no net change in sedimentation are distributed throughout the system (Fuller 1982; Jaffe and others 1998; Higgins and others 2005, 2007). This complex depositional history makes it difficult to capture a complete history of sediment deposition in San Francisco Bay at a single site. Three San Pablo Bay cores: Core 90-8, Rodeo Core, and Core 104 (Figure 1B) provide a composite depositional history where hydraulic mining debris can be contrasted with modern and pre-Gold Rush sediments. All three cores contain sediment deposited during recent times (~1900–1990). Two cores (90-8 and Rodeo) contain sediments deposited during the hydraulic mining period (1852–1884). One core (Rodeo) contains 5.4 m of sediment deposited before the major period of human activity that began with the Gold Rush (pre-1849).

Core 90-8

Core 90-8 is 240 cm long and >75% silt and clay. Laminations of silt, clay, and fine sand are evident throughout the core. Sandy layers are more prevalent between 110 cm and 170 cm. The maximum thickness for a sandy layer is approximately 5 cm. There is little evidence of bioturbation and shell material is sparse.

Core 90-8 was characterized in earlier studies (papers in van Geen and Luoma 1999), and it was determined that it does not extend into pre-Gold Rush sediment. The disappearance of unsupported ^{210}Pb below 120 cm suggests that sediment below this depth is at least 60 years old. Below 120 cm to the bottom of the core, unsupported ^{210}Pb, ^{137}Cs, and $^{239,240}Pu$ are all undetectable (Fuller and others 1999). Core reconstructions from the historical bathymetry model indicates that sediment between 110 cm and 268 cm was deposited during the time of hydraulic mining (Figure 3A). The model also suggests that between 1922 and 1951 erosion removed 104 cm of sediment and juxtaposed sediment deposited in 1883 with sediment deposited in 1951 at ~110 cm (Fuller and others 1999; Higgins and others 2007). This unconformity in the core correlates within 10 cm to the abrupt disappearance of unsupported ^{210}Pb, ^{137}Cs, and $^{239,240}Pu$. A maximum ^{10}Be activity at 212 cm also suggests that this core does not extend into sediment deposited before anthropogenic disturbance of the estuary (van Geen and others 1999) and may reflect some of the overburden disturbed in the mining process. These data are consistent with the suggestion that sediment below 120 cm to the bottom of the core at 240 cm was deposited during the hydraulic mining period (Figures 2 and 3). This sediment between 120 cm and 240 cm is grayish orange (10YR 6/2) when dried and shell material is nearly absent.

Above 120 cm, dried core samples are light olive grey (5 Y 5/2), shell material is more abundant, and sediment was deposited after 1952 (Figure 2A). In these upper layers, ^{210}Pb, ^{137}Cs, and $^{239,240}Pu$ are all present (Fuller and others 1999). An average sediment deposition rate for the last 40 years of 4 cm/yr was calculated from the radioisotope profiles. This is in contrast to a predisturbance sedimentation rate of 0.07 cm/yr determined for the estuary (van Geen and others 1999).

Rodeo Core

The Rodeo Core, collected in 1996, is 6.7 m long and consists of laminated fine sand, silt, clay, and shell-rich layers. It is coarser grained than cores 90-8 and 104 (50% to 75% silt and clay) and shell material is more abundant. The coarser grain size in the Rodeo Core suggests a higher energy environment, likely because of its proximity to the channel.

The Rodeo Core contains sediment deposited before the Gold Rush from 123 cm to the bottom of the core at 670 cm (Figure 2B). Below 123 cm, dried core sediment is olive grey (5 Y 4/1) and interspersed with shell layers down to the bottom of

the core. The ^{14}C ages on shells below 123 cm are 130 cm = 1670 yr BP, 208 cm = 1790 yr BP, 330 cm = 1980 yr BP, and 670 cm = 2130 yr BP (Ingram and others 1996). These ^{14}C ages and lack of metal contamination indicate that sediment below 123 cm was deposited before anthropogenic disturbance of the estuary. Hereafter in this paper, the Rodeo sediment below 123 cm will be referred to as pre-Gold Rush sediment or background values.

There is a noticeable transition in the Rodeo Core at 123 cm. Between 40 and 123 cm, dried sediment is grayish orange (10 YR 6/2), shell material is less abundant, and cross bedding and laminations are evident. Above 123 cm, *Macoma* and *Mya arenia* shells predominate. Below 123, a 20 cm thick shell layer contains mostly the native species *Mytilus edulis* (95%) and *Ostea lurida* shells. Ingram and others (1996) noted that the transition at 123 cm in the Rodeo Core is coincident with a strong seismic reflector in San Pablo Bay and may be the result of an extreme hydrologic event. We suggest that this transition is associated with the deposition of hydraulic mining debris.

Above 40 cm, the dried sediment color is a mix between the olive gray and grayish orange and shell material is abundant. ^{137}Cs was detected only in the uppermost interval analyzed (2-4 cm) and not in the 22-24 cm interval or below indicating the 1952 horizon occurs above 22 cm (Figure 2B). In contrast, the historical bathymetry model suggests that 1951 is at 49 cm (Figure 3B). This difference may be due in part to possible loss of surface sediment during the piston coring. The historical bathymetry model also suggests that sediment deposited during the time of hydraulic mining should extend from 49 cm to 240 cm (191 cm thick) (Figure 3B). The thicknesses of sediment deposition or erosion from the bathymetry model for this core are as follows: 1856–1887 = 221 cm, 1887–1898 = 36 cm, 1898–1922 = -5 cm, 1922–1951 = -61 cm, 1951–1983 = 37 cm, 1983–1993 = 12 cm. The ^{14}C date at 130 cm of 1670 BP indicates that hydraulic mining debris does not extend below 130 cm in the Rodeo Core. The geochemical data (see below) is consistent with the ^{14}C age at 130 cm and suggests that the hydraulic mining layer extends from ~40 to 123 cm (~83 cm thick).

Core 104

Core 104 is 192 cm long. There is a 6 cm sand layer at the bottom of the core (186-192 cm). The majority of the core between 50 and 186 cm is over 90% silt and clay. The upper 50 cm are coarser grained with up to 52% sand. The dried core sediments are light olive gray (5 Y 5/2).

Core 104 contains only sediment deposited after the hydraulic mining period. ^{137}Cs is present until 150 cm and peaks at 115 cm (Figure 2C). Assuming a constant sedimentation rate, the age at the bottom of the core at 192 cm is 1935. Historical bathymetry suggests that the age at the bottom of the core is approximately 1922 (Figure 3C). The thicknesses of sediment deposition or erosion from the bathymetry model for this core are as follows: 1887-1898 = 110 cm, 1898-1922 = 125 cm, 1922-1951 = 60 cm, 1951-1983 = 108 cm, 1983-1990 = 24 cm. All of Core 104 contains anthropogenic Pb and Hg contamination and does not extend into sediment layers that were deposited before anthropogenic influence on the estuary.

Accuracy of Historical Bathymetry

A key component of identifying hydraulic mining debris is the use of historical bathymetry to fill in identification of sediments deposited during times when radioisotopic identification is not possible. Thus, it is also worthwhile to explicitly consider how well the bathymetric reconstructions match geochemical indications of age. The disappearance of ^{137}Cs and the 1951 horizon predicted by historical bathymetry agree within 14 cm in Core 90-8. In Core 104, the two horizons are off by 18 cm. Poorer agreement was observed in the Rodeo Core where the disappearance of ^{137}Cs occurs between 4 and 22 cm. The bathymetry model predicts the 1951 horizon at 49 cm for a difference of as much as 45 cm. The navigational error on the core locations is ±100 m which introduces variation in depth estimates where the bay bottom is sloping. The combination of this variation and sounding error (Schallowitz 1964) results in uncertainty in the bathymetric reconstructions of up to ±25 cm. The maximum uncertainty on the 1952 horizon from ^{137}Cs dating is ±10 cm. In the

three San Pablo Bay cores, the range of difference of 14 to 45 cm between ^{137}Cs data and the historical bathymetry model is consistent with these combined uncertainties. However, the increased sedimentation rates (Jaffe and others 1998) and the estimated average of a 1 meter thick hydraulic mining horizon in the bay (Gilbert 1917), even a 45 cm uncertainty has proven useful in bounding sediment deposited during the time of hydraulic mining. The range of geochemical analyses consistently suggests that there is good agreement between the historical bathymetry predictions and changes in the geochemistry in Cores 90-8 and 104. In the Rodeo Core, the geochemical analyses suggest that the hydraulic mining debris is less thick and nearer to the surface than predicted by the historical bathymetry.

Hydraulic Mining Signature

The geochemical ranges for sediment deposited before, during, and after hydraulic mining are summarized in Table 2. The details are presented below.

Bulk Chemistry

A ternary Al_2O_3–CaO–K_2O plot indicates that San Pablo Bay core sediments trend between average shale (Krauskopf 1967; Taylor and McLennan 1985) and hydraulic mine sediments (Figure 4; Table 3). The core sediments that plot closest to the average shale values are the pre-Gold Rush sediments in the Rodeo Core and are considered background values. Sediments that plot closest to the sediment from the hydraulic mining source areas are core horizons deposited during the hydraulic mining period: horizons below 120 cm in Core 90-8, and horizons 62-63 cm and 102-103 cm in the Rodeo Core. Modern sediments deposited since 1952, span almost

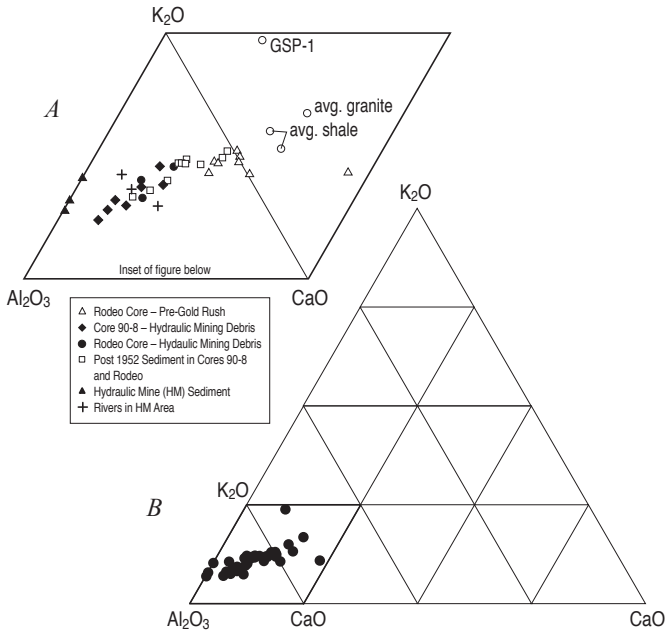

Figure 4 Ternary plots of selected geochemical constituents comparing bay sediments to average shale and hydraulic mine sediments. The bay sediment is higher in Al_2O_3 and lower in K_2O and CaO than average shale. Hydraulic mine sediments plot near the Al_2O_3 apex (solid triangles).

the entire range of the trend from background values to stream sediment in the hydraulic mine area suggesting a mixture of these sediment components and therefore continuing deposition of hydraulic mining sediment from the watershed and/or remobilized from within the bay.

The K_2O values are relatively constant in the core sediments, while CaO changes significantly (Figure 4). When Ca is ratioed to aluminum, a relatively immobile element, the pre-Gold Rush sediment in the Rodeo Core has Al/Ca ≤ 7.1. Shell rich layers in pre-Gold Rush horizons have the lowest Al/Ca (Al/Ca = 2.1) (Table 3). In contrast, sediment depos-

Table 2 Ranges of values in core sediment from San Francisco Bay

	εNd	$^{87}Sr/^{86}Sr$	Al/Ca	Ni/Zr	TOC (%)	Hg (ug g^{-1})
Post hydraulic mining	-3.32 to -5.50	0.7081 – 0.7092	5.0 – 8.5	1.24 – 1.76	1.1 – 1.7	0.16 – 0.79
Hydraulic mining debris	-4.64 to -7.10	0.7087 – 0.7103	7.8 – 18.9	0.77 – 1.15	0.5 – 1.0	0.09 – 0.45
Pre-Gold Rush	-2.65 to -4.02	0.7075 – 0.7086	2.1 – 7.1	1.11 – 1.30	0.9 – 1.4	0.03 – 0.08

Table 3 Geochemistry of stream bed sediment and bay core sediment

		Al/Ca	Ca/Sr	Zr/Hf	Ni/Zr	Fe (%)	Pb (ug g^{-1})	Hg (ug g^{-1})	Qtz/Plag
Rivers									
Steephollow Creek (at You Bet Pit)		12.6	62	37	0.90	4.39	13.7		
Greenhorn Creek		19.2	51	35	1.36	4.46	14.1		
Bear River at Wheatland		8.0	92	36	0.78	5.17	10.2		
Sacramento River #1a (near Verona)		4.8	113	37	1.35	5.02	10.7		
Sacramento River #1b (near Verona)		5.1	115	36	1.19	5.19	13.5		
SacramentoRiver #2 (near Hood)		5.2	118	36	1.24	5.00	12.0		
Old River (Hwy. 4 bridge)		5.0	73	35	0.87	5.17	38.2		
San Joaquin (Hwy. 4 bridge)		4.5	72	33	0.80	4.35	29.5		
Core 90-8									
0 - 2 cm		8.1	70	36	1.26	4.18	23.1	0.29	
9 - 10 cm		8.2	75	35	1.28	4.16	24.6	0.29	1.5
22 - 23 cm	shell rich layer	5.0	95	34	1.47	4.18	18.8	0.22	
29 - 30 cm		7.5	78	37	1.24	4.36	25.2	0.33	4.3
55 - 56 cm		7.2	78	37	1.30	4.23	31.7	0.36	
69 - 70 cm		7.7	76	36	1.32	4.43	39.1	0.42	
89 - 90 cm		7.9	81	36	1.24	4.52	42.5	0.46	3.3
92 - 93 cm		5.5	95	37	1.42	4.33	15.9		
109 - 110 cm		8.5	72	37	1.76	4.92	19.9		
114 - 117 cm	post-1952	8.2	70	33	1.52	4.60	50.6	0.70	
129 -130 cm		12.1	66	36	0.98	3.87	13.5	0.36	4.6
133 -134 cm		12.3	68	36	1.07	3.96	11.9	0.39	10.0
149 - 150 cm								0.38	
153 - 154 cm		10.0	65	36	0.96	4.60	13.8		11.8
169 - 170 cm		16.8	60	37	0.77	4.22	12.7		
189 - 190 cm		18.9	57	36	0.83	4.08	12.3	0.31	6.0
209 - 210 cm								0.35	
224 - 225 cm		10.6	68	34	1.14	5.53	12.8	0.31	
235 - 237 cm		11.1	74	33	1.15	4.40	12.9		
Core 104									
1 - 2 cm								0.33	
11 - 12 cm								0.20	
25 - 25 cm								0.42	
45 - 46 cm								0.36	
65 - 66 cm								0.26	
85 - 86 cm								0.40	
105 - 106 cm								0.55	
125 - 126 cm								0.64	
145 - 146 cm	post-1952							0.79	
165 - 166 cm								0.73	
185 - 186 cm								0.73	

Table 3 Geochemistry of stream bed sediment and bay core sediment (Continued)

		Al/Ca	Ca/Sr	Zr/Hf	Ni/Zr	Fe (%)	Pb (ug g^{-1})	Hg (ug g^{-1})	Qtz/Plag
Rodeo Core									
2 - 3 cm	post-1952	6.2	86	35	1.36	4.74	26.8	0.16	
143 - 144 cm	shell rich layer	3.8	103	35	1.14	4.42	9.5	0.06	
188 - 189 cm		5.2	90	34	1.25	5.05	8.9	0.04	2.79
260 - 261 cm		4.3	95	36	1.18	4.77	8.6	0.08	
360 - 361 cm	shell rich layer	2.1	138	35	1.20	4.71	8.5		
380 - 381 cm		7.1	92	34	1.12	4.83	8.5		
450 - 451 cm		4.3	95	35	1.15	4.38	7.9	0.06	
550 - 551 cm		6.5	93	34	1.20	4.87	8.8		
650 - 651 cm		4.5	90	35	1.29	5.04	8.9		
Other Background Values									
Richardson Bay									
119 - 120 cm		5.5	83	34	1.30	3.62	7.8	0.06	
130 - 131 cm		3.7	88	35	1.38	3.76	7.8	0.06	
139 - 140 cm		4.2	78	36	1.28	3.95	7.9	0.06	3.45
South Bay									
199 - 200 cm		6.3	81	36	1.11	4.50	8.6		
219 - 220 cm		6.5	80	36	1.11	4.59	8.2		
Grizzly Bay									
199 - 200 cm								0.03	3.31

ited during the hydraulic mining period in both the Rodeo Core and in Core 90-8 have the highest Al/Ca (Table 3), ranging from 7.8 to 18.9. In the modern sediments (post-1952), Al/Ca is 8.5.

Ca/Sr varies inversely with Al/Ca. The pre-Gold Rush sediments have the lowest Al/Ca and the highest Ca/Sr. In contrast, sediment deposited during the hydraulic mining period have the highest Al/Ca and lowest Ca/Sr (Tables 1 and 3). Al/Ca increases and Ca/Sr decreases in intervals deposited during the hydraulic mining period (Figure 5). These changes likely reflect a decrease in carbonate material relative to plagioclase feldspar.

In all the sediments analyzed, the consistent Zr/Hf suggests that there was complete dissolution of sample and that mineral fractionation was not significant (Table 3). Thus, trace elements ratioed to Zr, another relatively immobile element, can be used to normalize the data. Pre-Gold Rush sediment in the Rodeo Core, has Ni/Zr > 1.1 (Figure 6B; Table 3). Sediment deposited during the hydraulic mining period has Ni/Zr < 1.1 (Table 3) and should decrease Ni/Zr in bay sediment. Ni/Zr is decreased in sediment deposited during the time of hydraulic mining in both the Rodeo Core and Core 90-8 (Figure 6). Modern sediment has Ni/Zr values > 1.2 (Table 3) likely due to anthropogenic contamination.

The total organic carbon (TOC) in the core sediments follows Ca/Sr and Ni/Zr and decreases as Al/Ca increases. Thus, in both Core 90-8 and the Rodeo core, there is a decrease in TOC in sedi-

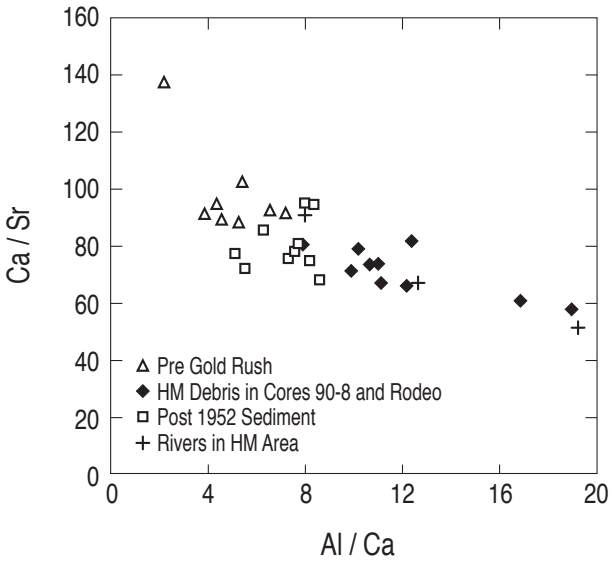

Figure 5 Ca/Sr versus Al/Ca illustrates the low Al/Ca and high Ca/Sr of pre-Gold Rush sediments and the change toward higher Al/Ca and lower Ca/Sr in sediments deposited during the time of hydraulic mining. Sediments containing more hydraulic mining debris plot closer to creeks and rivers in the hydraulic mining area.

ments deposited during the hydraulic mining period (Figure 7). Core sediments with TOC higher than 1.1% are olive gray. In contrast, core sediments deposited during the hydraulic mining period have TOC < 1.0% and are a grayish orange. However, Fe content in the olive gray and grayish orange sediment are similar (Table 3). Although the hydraulic mine sediments were not analyzed for TOC, it is likely that the mine sediments are depleted in C and also carbonate.

In summary, the major chemistry of sediments deposited in the bay during the hydraulic mining period is fundamentally different from the sediments deposited both before and after hydraulic mining occurred (Table 2, which summarizes these results). These differences reflect a disparity between undisturbed bay sediment and the chemistry of sediments in the hydraulic gold mining areas. Depending upon their depositional date, the bay sediments reflect mixing between the two sources. Compared to sediments that dominated deposition in the bay before hydraulic mining, high Al/Ca, low Ca/Sr, low Ni/Zr ratios, and

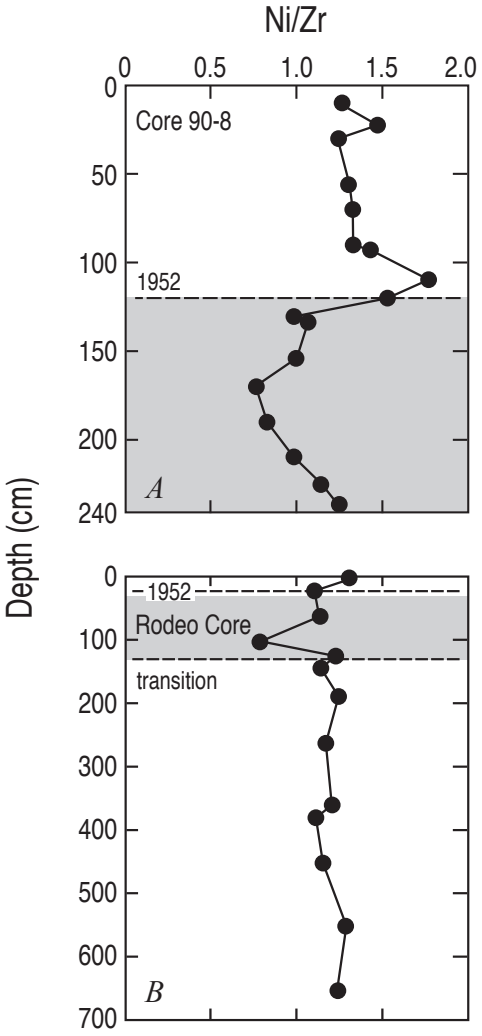

Figure 6 Profiles of Ni/Zr versus depth in sediment show Ni depletion in sediment deposited during the time of hydraulic mining (depicted by the gray shading)

low TOC concentrations all are characteristics of sediments containing hydraulic mining debris.

Mineralogy

The upper auriferous gravels that were hydraulically mined in the Sierra-Nevada predominantly consist of quartz clasts (Lindgren 1911; Gilbert 1917; Yeend 1974; James 1991a). Thus, bay sediment deposited during the time of hydraulic mining is expected to be enriched in quartz. X-ray diffractometry (XRD) results show that the ratio of quartz to plagioclase

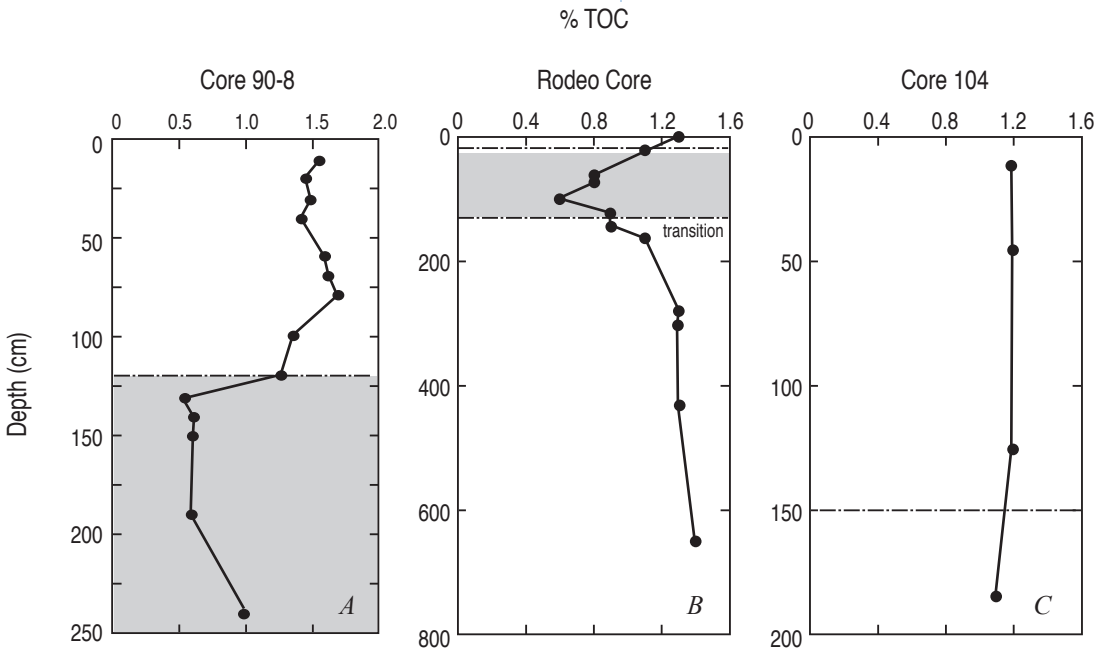

Figure 7 Profiles of TOC versus depth in sediment show TOC minima in sediment deposited during the time of hydraulic mining (depicted by the gray shading)

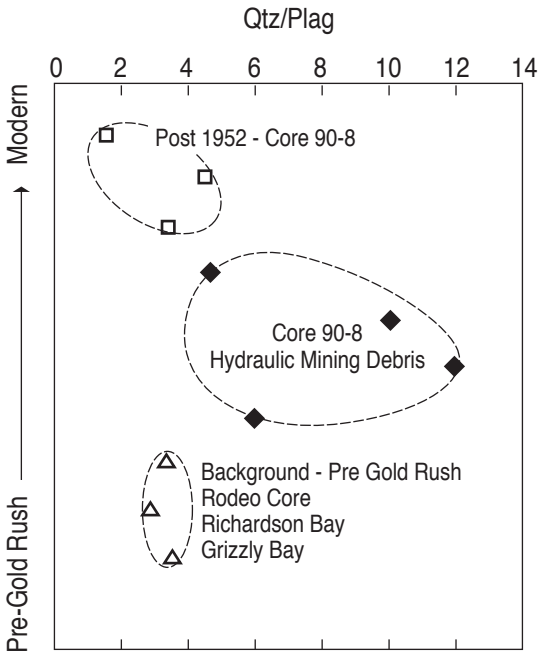

Figure 8 Quartz/plagioclase ratio in bay sediments determined from X-ray diffraction. In Core 90-8, sediment below 120 cm (sediment deposited during the time of hydraulic mining) has a higher quartz/plagioclase ratio than bay sediment deposited before hydraulic mining started (pre-Gold Rush) and after 1952 (upper 120 cm of Core 90-8).

of background sediment in the Rodeo Core is similar to pre-Gold Rush sediment in other nearby embayments (Grizzly Bay and Richardson Bay) (Figure 8). In Core 90-8, sediment deposited during hydraulic mining has higher quartz/plagioclase than pre-hydraulic mining sediment and modern sediment deposited after 1952.

Sr and Nd Isotopic Compositions

The most definitive characteristics of bay sediments that distinguish hydraulic mining debris from other sediment sources are the lithogenic isotope signatures. As noted earlier, sediments from the mine areas contain distinctly negative εNd values and elevated $^{87}Sr/^{86}Sr$ values as compared to historic (pre-Gold Rush) sedimentation in the bay.

The $^{87}Sr/^{86}Sr$ of pre-Gold Rush or background sediments are consistently below 0.7089 (Figure 9D). In sediments deposited during the hydraulic mining period, the $^{87}Sr/^{86}Sr$ values increase to a maximum of 0.71025. In Core 90-8, a board horizon of sediment deposited during the hydraulic mining period has $^{87}Sr/^{86}Sr > 0.7095$ and transition zones above

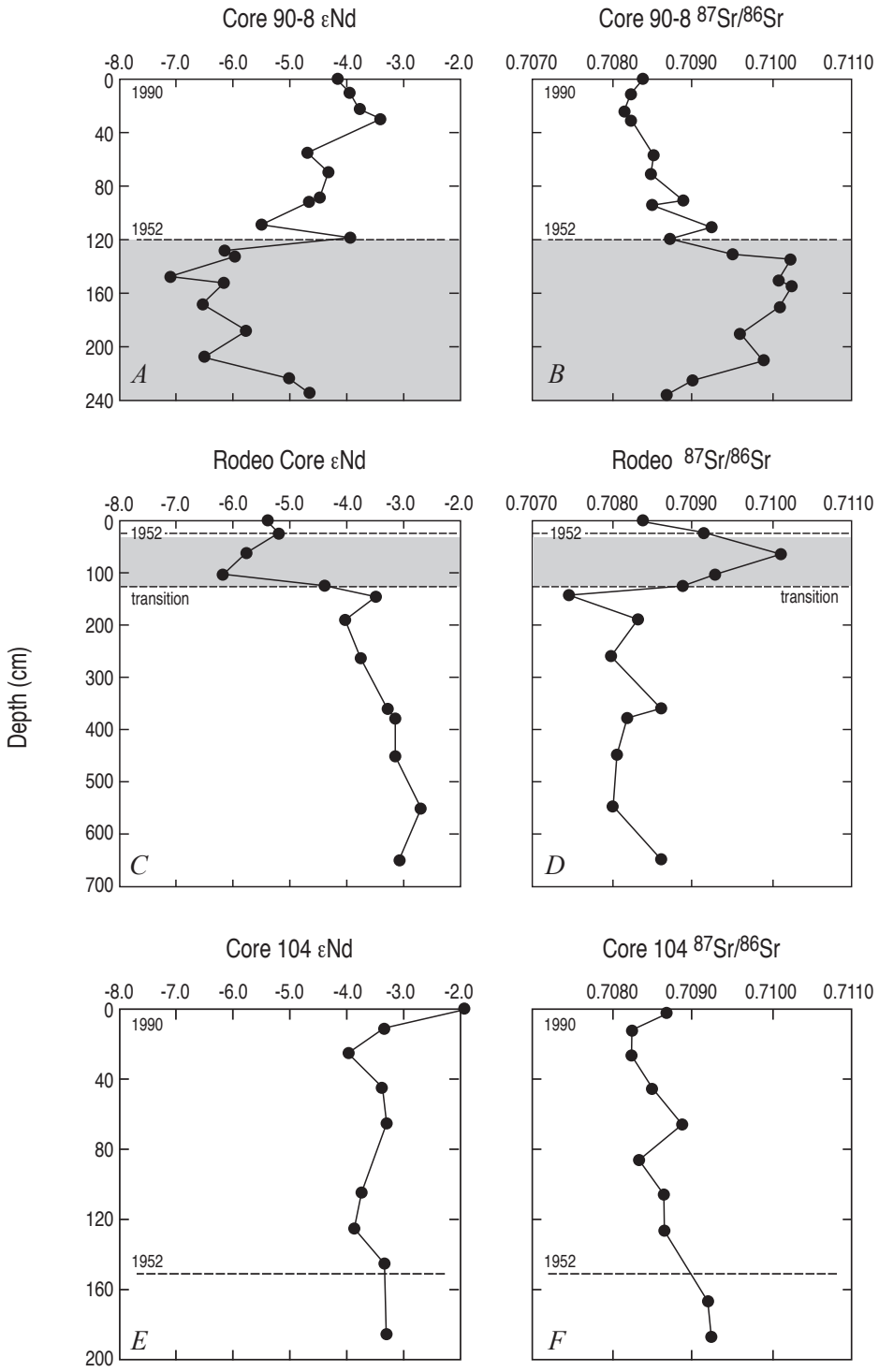

Figure 9 Profiles of εNd and $^{87}Sr/^{86}Sr$ versus depth in sediment show sediments deposited during the time of hydraulic mining have more negative εNd and higher $^{87}Sr/^{86}Sr$. Gray shading indicates hydraulic mining period.

and below where the $^{87}Sr/^{86}Sr$ values move toward the pre-Gold Rush values (<0.7089). In the Rodeo Core, the hydraulic mining layer $^{87}Sr/^{86}Sr$ values are similar to those in Core 90-8 ranging from 0.7091 to 0.7101. In post-1952 sediment, the $^{87}Sr/^{86}Sr$ is 0.7084 in the Rodeo Core, 0.7080 to 0.7092 in Core 90-8, and, 0.7082 to 0.7092 in Core 104 (Figure 9D, 9E, 9F; Table 4). In both Core 90-8 and Core 104, the $^{87}Sr/^{86}Sr$ values decrease toward the surface suggesting a decrease in hydraulic mining debris towards the surface.

The pre-Gold Rush $^{87}Sr/^{86}Sr$ values of 0.7075 to 0.7086 in the Rodeo Core (Figure 9D) are consistent with values found in old uncontaminated sediment in other bays within the estuary (0.7079 to 0.7082) (Table 4). The range of background $^{87}Sr/^{86}Sr$ values are consistently higher than $^{87}Sr/^{86}Sr$ values bed sediment in the Sacramento and San Joaquin rivers (0.7061 and 0.7072, respectively; samples taken ~50 km upstream of where each river meets the bay, salinity = 0) (Figure 1; Table 3). This suggests that interaction and exchange between Sr of oceanic ori-

Table 4 Sr and Nd concentrations and isotopic ratios of stream bed sediment and bay core sediment

		Sr (ug g^{-1})	Nd (ug g^{-1})	$^{87}Sr/^{86}Sr$	$^{143}Nd/^{144}Nd$	εNd
Rivers						
Steephollow Creek (at You Bet Pit)		80	24.2	0.71174 (1)	0.512188 (09)	-8.74
Greenhorn Creek		62	25.6	0.70967 (1)	0.512272 (11)	-7.10
Bear River at Wheatland		90	20.6	0.70692 (1)	0.512321 (15)	-6.14
Napa River (Hwy. 29 bridge)				0.70782 (1)	0.512530 (09)	-2.07
Sacramento River #1a (near Verona)		114	14.5	0.70603 (1)	0.512504 (10)	-2.56
Sacramento River #1b (near Verona)				0.70613 (1)	0.512505 (12)	-2.55
Sacramento River #2 (near Hood)		120	16.0	0.70629 (1)	0.512445 (11)	-3.73
Old River (Hwy. 4 bridge)		174	19.2	0.70766 (1)	0.512408 (09)	-4.45
Middle River (Hwy. 4 bridge)				0.70727 (1)	0.512350 (12)	-5.57
San Joaquin River (Hwy. 4 bridge)		214	21.3	0.70723 (1)	0.512346 (09)	-5.66
Core 90-8						
0 - 2 cm		105	15.0	0.70836 (1)	0.512421 (14)	-4.20
9 - 10 cm		106	14.8	0.70821 (2)	0.512431 (09)	-3.99
22 - 23 cm		91	14.5	0.70813 (1)	0.512457 (12)	-3.50
29 - 30 cm		92	14.2	0.70821 (1)	0.512461 (10)	-3.41
55 - 56 cm		96	14.3	0.70850 (1)	0.512395 (13)	-4.70
69 - 70 cm		100	14.9	0.70846 (2)	0.512414 (20)	-4.33
89 - 90 cm		91	16.0	0.70888 (1)	0.512405 (11)	-4.50
92 - 93 cm		104	16.2	0.70848 (2)	0.512396 (17)	-4.68
109 - 110 cm		97	15.3	0.70924 (3)	0.512354 (10)	-5.50
115 - 117 cm	post-1952	95	16.5	0.70871 (1)	0.512433 (15)	-3.96
129 - 130 cm		89	16.7	0.70950 (1)	0.512320 (14)	-6.16
133 - 134 cm		66	17.9	0.71023 (1)	0.512330 (12)	-5.97
149 - 150 cm				0.71008 (1)	0.512272 (14)	-7.10
153 - 154 cm		67	17.0	0.71025 (1)	0.512320 (24)	-6.16
169 - 170 cm		71	18.4	0.71010 (1)	0.512317 (07)	-6.22
189 - 190 cm		82	17.9	0.70960 (1)	0.512341 (33)	-5.75
209 - 210 cm				0.70990 (1)	0.512322 (10)	-6.12
224 - 225 cm		99	19.9	0.70900 (1)	0.512379 (10)	-5.01
235- 237 cm		95	17.0	0.70868 (2)	0.512398 (17)	-4.64

Table 4 Sr and Nd concentrations and isotopic ratios of stream bed sediment and bay core sediment (Continued)

		Sr (ug g^{-1})	Nd (ug g^{-1})	$^{87}Sr/^{86}Sr$	$^{143}Nd/^{144}Nd$	εNd
Core 104						
1 - 2 cm				0.70863 (1)	0.512449 (20)	-3.65
11 - 12 cm				0.70820 (1)	0.512462 (10)	-3.39
25 - 25 cm				0.70820 (1)	0.512430 (13)	-4.00
45 - 46 cm				0.70847 (1)	0.512461 (10)	-3.41
65 - 66 cm				0.70884 (1)	0.512466 (10)	-3.32
85 - 86 cm				0.70830 (2)		
105 - 106 cm				0.70862 (1)	0.512443 (14)	-3.76
125 - 126 cm				0.70861 (1)	0.512437 (07)	-3.88
145 - 146 cm					0.512464 (11)	-3.36
165 - 166 cm				0.70916 (1)		
185 - 186 cm				0.70920 (2)	0.512466 (09)	-3.32
Rodeo Core						
2 - 3 cm	post-1952	110	18.8	0.70843 (2)	0.512358 (13)	-5.38
22 - 23 cm		103	19.6	0.70914 (2)	0.512370 (10)	-5.18
62 - 63 cm		94	17.2	0.71011 (4)	0.512341 (11)	-5.75
102 - 103 cm		101	19.2	0.70927 (2)	0.512321 (13)	-6.07
123 - 124 cm	transition	116	17.1	0.70887 (1)	0.512411 (22)	-4.39
143 - 144 cm	shell rich layer	168	15.1	0.70746 (3)	0.512458 (11)	-3.47
188 - 189 cm		129	16.4	0.70832 (4)	0.512430 (14)	-4.02
260 - 261 cm		132	16.1	0.70798 (5)	0.512444 (16)	-3.74
360 - 361 cm	shell rich layer	171	14.2	0.70862 (3)	0.512469 (09)	-3.25
380 - 381 cm		117	14.4	0.70818 (2)	0.512476 (07)	-3.12
450 - 451 cm		127	15.0	0.70805 (2)	0.512476 (08)	-3.12
550 - 551 cm		120	15.0	0.70800 (2)	0.512499 (10)	-2.67
650 - 651 cm		122	14.7	0.70861 (2)	0.512480 (08)	-3.04
Other Background Values						
Richardson Bay						
119 - 120 cm		118	11.1	0.70785 (1)	0.512448 (09)	-3.66
130 - 131 cm		110	11.6			
139 - 140 cm		116	11.8	0.70793 (1)		
South Bay						
199 - 200 cm		109	14.5	0.70815 (4)		
219 - 220 cm		106	15.7			
Grizzly Bay						
199 - 200 cm				0.70802 (2)	0.512500 (10)	-2.65

gin (seawater $^{87}Sr/^{86}Sr$ = 0.70906) and the terrestrially derived Sr in the sediments could cause such a shift to higher values. An experiment was performed using ammonium acetate extraction (see methods section) to determine if the exchangable fraction of Sr in the sediment contained more of an oceanic than a terrestrial Sr signature (Table 5). Sr exchange was determined for three samples from the bay cores, one river bed sediment, and one hydraulic mine sediment (Table 5). The $^{87}Sr/^{86}Sr$ of supernatants from the three bay sediments increased from their original composition and shifted toward a seawater value. In these three supernatants, there was also a decrease in Ca/Sr and an increase in Na/Ca that are consistent with seawater exchange. In contrast, the $^{87}Sr/^{86}Sr$ of the supernatants from the Sacramento River sample and the Gold Run hydraulic mine sample changed little from the original composition of the sediment.

While seawater and carbonate material increase the $^{87}Sr/^{86}Sr$ of pre-Gold Rush sediment, they could decrease the $^{87}Sr/^{86}Sr$ of sediment released from the hydraulic mines. Hydraulic mine sediment has $^{87}Sr/^{86}Sr$ values that range between 0.7105 and 0.7455 (Table 1). In the cores where sediment is interpreted to have been deposited during the time of hydraulic mining, the $^{87}Sr/^{86}Sr$ is higher than the seawater value of 0.7092. These higher Sr isotopes correlate with the more negative εNd values and suggest that although the $^{87}Sr/^{86}Sr$ may have been low-

Table 5 Exchange experiment results

	Sediment Sr (ug g^{-1})	Supernate Sr (ug g^{-1})	Residue Sr (ug g^{-1})	% in Supernate	% in Residue	Total %
Rodeo, 380 - 381 cm	117	31	76	26%	65%	91%
Richardson Bay, 130 - 131 cm	110	28	82	25%	75%	100%
Core 90-8, 153 - 154 cm	67	14	58	21%	87%	107%
Sacramento River #2	120	20	90	17%	75%	92%
Gold Run #2 (near monitor)	23	3	17	13%	74%	87%
	Ca/Sr	**Ca/Sr**	**Ca/Sr**			
Rodeo, 380 - 381 cm	92	63	88			
Richardson Bay, 130 - 131 cm	90	70	84			
Core 107, 153 - 154 cm	71	61	70			
Sacramento River #2	113	106	113			
Gold Run #2 (near monitor)	8	8	8			
	Na/Ca	**Na/Ca**	**Na/Ca**			
Rodeo, 380 - 381 cm	0.70	1.59	0.39			
Richardson Bay, 130 - 131 cm	1.61	3.87	0.68			
Core 90-8, 153 - 154 cm	2.16	4.99	0.89			
Sacramento River #2	0.47	0.02	0.51			
Gold Run #2 (near monitor)	1.99	0.42	2.38			
	$^{87}Sr/^{86}Sr$	**$^{87}Sr/^{86}Sr$**	**$^{87}Sr/^{86}Sr$**			
Rodeo, 380 - 381 cm	0.70806	0.70907	0.70784			
Richardson Bay, 130 - 131 cm	0.70783	0.70909	0.70734			
Core 90-8, 153 - 154 cm	0.71025	0.70880	0.71079			
Sacramento River #2	0.70613	0.70601	0.70614			
Gold Run #2 (near monitor)	0.71804	0.71834	0.71796			

ered by seawater exchange, they still reflect hydraulic mines as a probable source. However, the isotopic exchange process does limit the use of Sr isotopes and concentrations for determining the fraction of hydraulic mining debris in the core layers.

Nd isotopes should be a more reliable indicator of sediment sources (Linn and others 1992). Nd and its radiogenic parent Samarium (Sm) are rare earth elements and the Sm/Nd is similar in most minerals. As a result, the parent to daughter ratio in sediments is not easily changed by weathering, sorting, or diagenesis. Thus, for the most part, Nd isotope ratios are independent of grain size (Goldstein and others 1984; Frost and Winston 1987; DePaolo 1981; McLennan and others 1989; Linn and others 1992). Also, seawater interaction is not as much of a concern because of the low Nd concentration in seawater compared to the sediment Nd concentrations. In the Rodeo Core, the pre-Gold Rush sediments have Nd concentrations that range from 14.2 to 16.4 μg g^{-1} and $^{144}Nd/^{143}Nd$ isotopic ratios that range from 0.512499 to 0.512430. The εNd values range from -2.67 to -4.02, respectively. In contrast, in Rodeo core sediments deposited during the hydraulic mining period, Nd concentrations increase and range between 17.9 and 19.2 μg g^{-1}, and εNd values decrease and range between -5.18 to -6.07 (Figure 9C; Tables 3, 4).

In Core 90-8, sediment deposited during the time of hydraulic mining has εNd values that range from -4.64 to -7.10 and Nd concentrations between 16.7 and 18.4. There is a broad horizon of sediment with εNd between -5.97 and -7.10, away from which the εNd values move toward baseline sediment values near the bottom of the core. The εNd of sediment deposited after 1952 increases toward the surface from -5.5 to a series of values between -4.20 and -3.41. Similarly, the more modern sediments in Core 104 have εNd between -4.00 and -3.32 (Figure 9A, 9C, 9E; Table 4).

An $^{87}Sr/^{86}Sr$ versus εNd plot shows that the bay sediments are offset in $^{87}Sr/^{86}Sr$ from the Sacramento and San Joaquin River bed sediment toward the $^{87}Sr/^{86}Sr$ of seawater (Figure 10). The εNd of background sediment in the Rodeo Core ranges between -2.7 and -4.0. Background samples plot between the present day values of seawater and the Sacramento River bed sediment (Figure 10).

The εNd background values in the Rodeo Core, suggest that: (1) in the past, either the εNd of San Joaquin River sediment was less negative or that San Joaquin input into San Pablo Bay was insignificant compared to the Sacramento; and/or (2) sediment input from the Napa and perhaps Petaluma rivers was more significant in the past than it is today; and/or, (3) the εNd of Sacramento River bed sediment is more negative today than it was in the past. It is likely that between the hydraulic mining areas and the bay, hydraulic mining debris increased the isotopic values of sediments stored in the tributary streambeds and banks (in the watershed) and in the bay.

The hydraulic mine sediment data plot at the opposite end of the εNd versus $^{87}Sr/^{86}Sr$ diagram from background bay sediment, with more negative εNd and higher $^{87}Sr/^{86}Sr$ (Figure 10). River sediment data in the hydraulic mine areas are offset from the mine sediment data suggesting that they not only contain mine sediment but a mix of other rock units in the watershed. In Core 90-8, data for sediment deposited during hydraulic mining plot away from background sediment data toward the hydraulic mining field, except for one sample at the bottom of the core (horizon 235-237 cm). Rodeo Core sediment deposited during hydraulic mining period has εNd values (-5.2 to –6.1) within the range of values from that period in Core 90-8. In Core 90-8, the εNd values begin to change back toward background values toward the surface. Few samples reach either the end member background values or hydraulic mine values. This is also true for Core 104 sediments. In the Rodeo Core, the εNd values do not decrease and suggest that the post 1952 sediment at this location contains a large component of redeposited hydraulic mining debris sediment. All three cores indicate that to varying degrees there has been remobilization and redeposition of the hydraulic mining debris within the bay. Remobilization and redeposition of sediment and contaminants within the bay has been previously shown with Pb isotopic ratios (Ritson and others 1999).

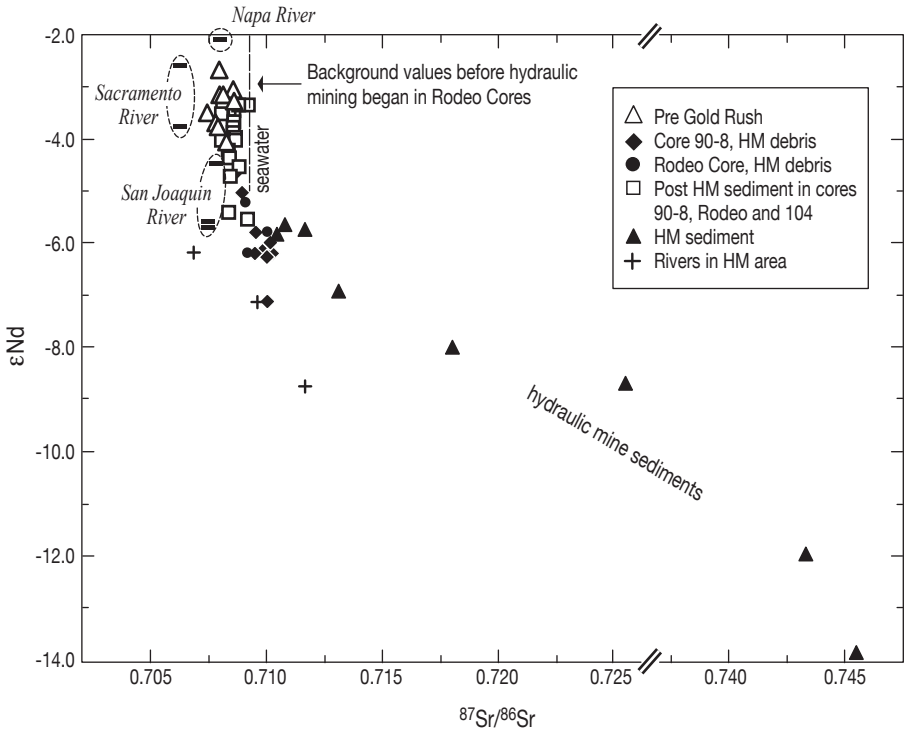

Figure 10 Plot of εNd versus $^{87}Sr/^{86}Sr$ illustrates the isotopic mixing among end members. Bay sediment background end member, the pre-Gold Rush sediment in bay cores, has εNd between -3 and -4 and $^{87}Sr/^{86}Sr$ between 0.7075 and 0.7086. Another end member, sediment in abandoned hydraulic gold mines, has εNd between -6 and -14 and $^{87}Sr/^{86}Sr$ between 0.7105 and 0.7455. Core sediment deposited in the bay during the time of hydraulic mining time has isotopic values that plot in the hydraulic gold mine field. Sr exchange with seawater shifts core sediments away from river sediment toward the seawater $^{87}Sr/^{86}Sr$ value. Core sediments deposited during the time of hydraulic mining and that contain larger amounts of hydraulic mining debris have $^{87}Sr/^{86}Sr$ higher than seawater. Isotopic values for core sediments deposited after hydraulic mining stopped are between the values of sediment deposited during hydraulic mining and background values.

Other Characteristics of Hydraulic Mining Debris in Bay Sediments

Once sediment intervals containing hydraulic mining debris were identified by their dates of deposition and their geochemical and isotopic similarity to mine and river sediments in the hydraulic mining areas, other general characteristics of those sediments became evident. There is a color change in the sediment from olive grey to grayish orange that accompanies the geochemical and isotopic changes that are consistent with hydraulic mining debris as the source. In the hydraulic mining areas the upper gravels are weathered to orange hues in many places. In the cores, the background sediment with the darkest olive grey sediment has the highest TOC and highest visible shell content. Because hydraulic gold mining was the first large-scale anthropogenic endeavor in the bay area watershed, it makes sense that the first shift from the background olive grey to grayish orange sediment was likely caused by hydraulic mining.

The sparse amount of shell material and low TOC are also consistent because hydraulic mine debris would not contain shells and organic material in abundance. Large increases in sedimentation rate would make it hard for some benthic animals to survive. The core sediment deposited during the time of hydraulic mining is laminated and shows little evidence of bioturbation. Not only is the shell material sparse but the type of shells found also changes. In pre-hydraulic mining sediment, the predominate bivalves are oyster and mussel shells. After hydraulic mining started, mussel shells are no longer present in the cores. It

is likely that the onset of hydraulic mining and the increased sedimentation in the bay caused the mussels to no longer thrive.

In the interpreted hydraulic mining debris in Core 90-8 there is an increase in grain size upcore from 240 cm to 120 cm. There are more sandy layers between 120 and 170 cm than between 170 and 240 cm. By comparison, the Core 90-8 interval between 120 and 170 cm has the lowest εNd, TOC, and Ni/Zr and, the highest $^{87}Sr/^{86}Sr$, Al/Ca, and quartz/plagioclase, all of which are characteristic of the mine material. This coarsening upward sequence is consistent with a shallowing of the bay from hydraulic mining debris. It is also likely that fine-grained material from the hydraulic mine area washed into the bay in greater proportions earlier in the history of hydraulic mining. Fine-grained material could easily be carried in suspension in water overflowing sluices and rapidly make its way downstream, while the heavy and/or coarse-grained material sank to the bottom of the sluice and was either taken away for gold separation or dumped nearby. Soil in the area disrupted by both road building and hydraulic mining, contains fine-grained material that the miners would have rapidly washed away. As time went on, higher proportions of the coarse-grained material may have made its way to the bay.

Estimates of Hydraulic Mine Sediment Percentage in Bay Sediments

Because Nd isotopes the most reliable indicator of sediment source, we used them to calculate the fraction of hydraulic mining debris mixed into the core sediment. The following mixing equation is used:

$$\varepsilon Nd_{mix} = \frac{(\varepsilon Nd)_B (Nd_B)(1-f) + (\varepsilon Nd)_{HM} (Nd_{HM})(f)}{(Nd_{mix})} \quad (1)$$

where εNd_B = the average background (pre-hydraulic mining) sediment, εNd_{HM} = the average hydraulic mine sediment, εNd_{mix} = the mixture in the bay sediments, and f = fraction of hydraulic mine debris in the core sediments. Nd_B, Nd_{HM}, and Nd_{mix} represent the Nd concentration of these components, respectively. Because the relative contribution of each mine is unknown, the average Nd signature from all mines sampled was used to represent the hydraulic mine sediment. The average calculated for εNd of the hydraulic mines is -8.38 μg g^{-1} (±2.90) and average Nd concentration is 20.56 μg g^{-1} (±3.15), where ± is the standard deviation. The average εNd of pre-Gold Rush sediments was calculated using background sediment values in the Rodeo core (below 143 cm), and also background sediments in Richardson Bay, South Bay and Grizzly Bay. The average εNd, for pre-Gold Rush sediment is -3.27 (±0.44) and the average Nd concentration is 14.28 μg g^{-1} (±1.71). Using these average values for mine source and pre-mining background, the fraction of hydraulic mine sediment, f, in each core interval was determined. The uncertainty in f was calculated by propagating the uncertainty defined by the standard deviation for each component through Equation 1. For sediment intervals deposited during the time of hydraulic mining, the maximum hydraulic mine material contribution is 54% in Core 90-8 and 56% in the Rodeo Core (Table 6). These results suggest that the hydraulic mine signature was diluted by other sediment transported downstream during the hydraulic mining period and from sedimentary processes within the bay. In post-1952 sediment, there is a maximum of 30% of the mining material in Core 90-8 and 43% in the Rodeo Core. The results suggest that modern sediment inputs diluted the hydraulic mining signature, but to various degrees depending upon location and that a significant amount of hydraulic mining debris remains in surface sediment. Surface sediment at the Core 90-8 location contains 10% hydraulic mining debris and at the Rodeo Core location surface sediments contain 43% hydraulic mining debris.

Protocol for Identifying Hydraulic Mining Debris

Since there is concern that hydraulic mining debris could be an important source of mercury contamination in water bodies downstream from the mines, a protocol is necessary to identify such sediments. In San Francisco Bay, a primary characteristic of sediments deposited during hydraulic mining is that they do not contain unsupported ^{210}Pb or ^{137}Cs. Likewise, they are too young to be dated by ^{14}C. The window constrained by radionuclides was broader than the

Table 6 Percent hydraulic mining debris bay core sediment

		% of Hydraulic Mining Debris	Error (±)
Core 90-8			
0 - 2 cm		13	10
9 - 10 cm		10	8
22 - 23 cm		3	7
29 - 30 cm		1	7
55 - 56 cm		16	11
69 - 70 cm		14	10
89 - 90 cm		20	12
92 - 93 cm		23	14
109 - 110 cm		30	17
115 - 117 cm	post-1952	15	10
129 - 130 cm		45	24
133 - 134 cm		48	26
153 - 154 cm		46	25
169 - 170 cm		54	29
189 - 190 cm		45	24
224 - 225 cm		42	23
235 - 237 cm		26	15
Rodeo Core			
2 - 3 cm	post-1952	43	24
22 - 23 cm		44	24
62 - 63 cm		42	23
102 - 103 cm		56	30
123 - 124 cm	transition	23	14

period of deposition, however, geochemical parameters coupled to sediment ages constrained by the bathymetry model and radioisotopes were used to define time horizons in cores to within 50 cm.

Sediments deposited during the mining period are not from hydraulic mining alone; and sediments deposited after that period likely contain mine debris mixed in some proportion. Separating the contribution of mining required a suite of analyses. The analyses should be conducted at different levels of screening to avoid unnecessary expense. The first signs of a high proportion of mining debris are an orange grey color, sparse shell material, laminations, and little bioturbation. These signal a rapid increase in sedimentation rate that inhibited biological productivity and low TOC.

Second order analyses should be X-ray diffraction to determine increase in quartz content, accompanied by analyses of major elements and trace elements. These approaches identify geologic/geochemical anomalies that differentiate the characteristics of the gold deposits from sediments typical of the bulk of the watershed. In San Francisco Bay, the anomalies are low TOC, low Ni, high Al, and low Ca concentrations that provide indicators of hydraulic mine sediment. Some of these parameters were used to calculate the percent of hydraulic mining debris for comparison to results from using the Nd signature. Reasonable agreement to f only was found for Ca/Sr, such that it could provide a screening tool for choosing intervals for measuring Nd isotopes (Figure 11).

None of the above traits, however, are unique to hydraulic mining debris. Anomalies could have other sources. But if those traits are present, a multi-isotopic approach provides the most convincing evidence, although time-consuming and expensive. Nd isotopic composition is the least susceptible to interferences (most reliable), but is also the most expensive and time-consuming analyses. When Nd analyses are supported by Sr analyses, and the visual and geochemical characteristics are present, the signature of the debris can be convincingly demonstrated; and the

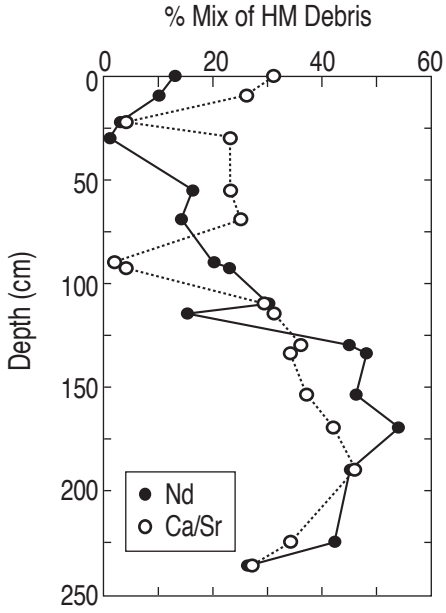

Figure 11 Comparison of the percent hydraulic mining debris versus depth for core 90-8 calculated using εNd and Ca/Sr

degree of contamination determined.

Because each characteristic alone or even several characteristics together can be indicative of other sediment sources, it is not hard to imagine why hydraulic mining debris had not been identified in bay cores before now; even though earlier studies suggested it had to be present and even estimated deposition, based on sediment transport (Gilbert 1917). The present study suggests that not only do deposits of one meter depth estimated by Gilbert (1917) occur in the bay but that mine debris continues to be transported into the bay, remobilized, and mixed into surface sediments. Our data suggest that the input of hydraulic mining debris is decreasing with time, but the legacy of 30 years of hydraulic mining remains a strong component of bay sediments, despite the cessation of mining more than 130 years ago.

Mercury in Bay Cores

Mercury concentrations in pre-Gold Rush sediment range between 0.04 and 0.08 µg g^{-1} (see also Hornberger and others 1999). Mercury concentrations higher than background values occur in both Cores 90-8 and Rodeo in sediment deposited during the time of hydraulic mining. The mercury concentrations are as high as 0.45 µg g^{-1} in the hydraulic mining layers but more commonly range between 0.3 and 0.4 µg g^{-1} (Figure 12). In post-1952 bay sediment, in some areas (like Grizzly Bay) mercury concentrations as high as 1.0 µg g^{-1} have been reported (Hornberger and others 1999). In Cores 90-8 and 104, the highest mercury concentrations occur around 1952 and then decrease toward the surface. The isotopic and geochemical indicators of hydraulic mining debris in the bay suggest that it is not a large component of these layers and that the mercury likely has more than one source. These higher mercury concentrations are probably related to the onset of mechanized mercury mining in the bay area.

Despite the distance for mercury transport from the Sierras across the Central Valley and into the bay (>200 km), it is clear that an enormous increase in sediment input into the bay occurred during the hydraulic mining period (Gilbert 1917; Jaffe

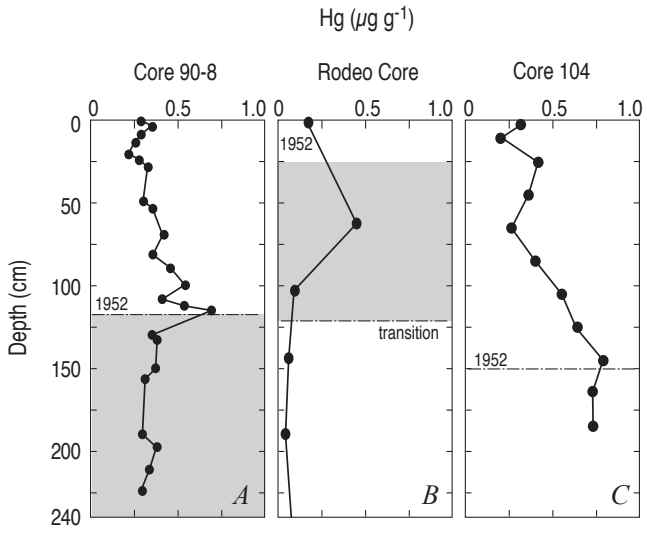

Figure 12 Profiles of sediment mercury concentration versus depth for cores 90-8, 104, and Rodeo

and others 1998) with some mercury transported with it. The historical bathymetry estimates that over 400,000,000 m^3 of sediment was deposited in north San Francisco Bay (San Pablo and Grizzly bays) between 1856 and 1887. The average mercury concentration in (dried) sediment deposited during that time is ~0.4 µg g^{-1} or 4.0 x 10^{-7} g. Assuming an average bulk density of 1.1 g cm^{-3} for the 400,000,000 m^3 of wet sediment, the amount of mercury deposited in the bay is approximately 176 tonnes. It is estimated that 40,000 tonnes of mercury were used in the Sierra Nevada gold-mining, and that 25% of it was lost to the environment (Nriagu 1994). Thus, potentially 10,000 tonnes of mercury could have reached the bay. Our calculations suggest that <2% of the mercury that was lost to the environment was present in the bay in 1990. Schoellhamer (2009) suggested that erosion of the bed sediments in the bay had depleted the erodible bed sediment pool in the bay by 1999, suggesting at least some of the mercury input from mining could have been lost to the ocean. Nevertheless, it seems likely there is considerable mercury left in the watershed, beyond the many tonnes of mercury that have already reached the bay. Identification and control of those deposits is an important goal for the future.

CONCLUSIONS

Sediment deposited in San Pablo Bay during the time of large-scale hydraulic gold mining in the Sierra Nevada (1852–1884) is geochemically different from earlier deposited sediment. A combination of radioisotopic age dating, visual characteristics, geochemical analyses, mineralogy, and isotopic compositions provide a set of parameters that are internally consistent with hydraulic mining being a large component of sediment deposited during this period. This general protocol should be useful in any depositional system suspected of receiving large sediment loads from such mining.

Sediment deposited after hydraulic mining stopped can still contain a significant fraction of hydraulic mining debris. The persistence of this material in surface sediments is due in part to remobilization and redeposition within the bay and in part to sediment stored in the rivers and flood plains that are still recovering from the deposition of enormous quantities of hydraulic mine sediments (Gilbert 1917; James 1989, 1991b). Because of the sheer volume of hydraulic mining debris containing mercury that has been released into the watershed, much of this material that remains in the Sierra piedmont (James 1989) is of great concern.

In San Francisco Bay, core intervals containing hydraulic mining debris have mercury concentrations of 5 to 10 times background levels. The combination of 400,000,000 m^3 of mercury contaminated hydraulic mining debris and the more recent mercury contamination in bay sediment potentially poses ecological risks for San Francisco Bay. Much of San Pablo Bay is eroding today (Jaffe and others 1998). Erosion in and around San Pablo Bay may expose horizons with higher mercury concentrations. Restoration of wetlands created by hydraulic mining debris may attract biota to areas with increased mercury methylation. A related concern is that the dynamic processes that result in the persistence of hydraulic mining debris in recently deposited sediments indicates that other particle bound contaminants will persist in surface sediments for many years after inputs cease, consistent with other findings in the bay for Pb (Ritson and others 1999; Steding and others 2000) and PCBs (Davis 2004).

Our estimates indicate that only 2 to 5 percent of the mercury lost during the hydraulic mining process is retained in San Francisco Bay. Some of this mercury could have been carried out to sea, but there is also potentially much mercury that remains in the streams and river beds upstream. Some of it is known to have been left behind in the mine sites (Hunerlach and others 1999) and some may reside in reservoir sediment behind dams (Alpers and others 2005). In any dam removal, the possibility of encountering mercury-laden sediments should be considered, with concomitant implications for the bay.

Primitive mining practices such as those used during the Gold Rush in the Sierra Nevada have or are currently being used in many parts of the world. The effects of such mining practices can be far reaching. In this paper, using a combination of techniques, mercury-laden sediment was traced over 250 km from its historic source. The geochemical indicators presented may be useful in other mining areas where comparable contamination is suspected in the watershed.

ACKNOWLEDGEMENTS

This paper was greatly improved by the reviews of Mike Singer, Jim Hein, Tom Bullen, and two anonymous journal reviewers. We would like to thank Lynn Ingram, Jim Ingle, and Roberto Anima for providing the bay cores. Also, assistance and consultation by Tom Bullen and John Fitzpatrick in their isotope laboratory was invaluable.

REFERENCES

Alpers CN, Hunerlach MP, May JT, and Hothem RL. 2005. Mercury contamination from historical gold mining in California. U.S. Geological Survey Fact Sheet 2005-3014.

Bullen TD and Clynne MA. 1990. Trace element and isotopic constraints on magmatic evolution at Lassen Volcanic Center. Journal of Geophysical Research 95(B):9671-9691.

Bullen T, White A, Blum A, Harden J, and Schulz M. 1997. Chemical weathering of a soil chronosequence on granitoid alluvium: II. Mineralogic and isotopic constraints on the behavior of strontium. Geochimica Cosmochimica Acta 61:291-306.

Conaway CH, Black FJ, Grieb TM, Roy S, and Flegal AR 2008. Mercury in the San Francisco Estuary. Reviews of Environmental Contamination and Toxicology 194:29–54.

Conomos TJ, editor. 1979. San Francisco Bay: the urbanized estuary. San Francisco (CA): American Association for the Advancement of Science, Pacific Division. 254 p.

Davis J. 2004. The long-term fate of PCBs in San Francisco Bay. Environmental Toxicology and Chemistry 23:2396-2409.

Davis JA, May MD, Greenfield BK, Fairey R, Roberts C, Ichikawa G, Stoelting MS, Becker JS, Tjeerdema RS. 2002. Contaminant concentrations in sport fish from San Francisco Bay, 1997. Marine Pollution Bulletin 44:1117-1129.

Davis JA, Yee D, Collins JN, Swartzbach SE, Luoma SN. 2003. Potential for increased mercury accumulation in the estuarine food web. San Francisco Estuary and Watershed Science [Internet]. Available from: http://www.escholarship.org/uc/item/9fm1z1zb.

Davis JA, Greenfield BK, Ichikawa M, Stephenson M. 2008. Mercury in sport fish from the Sacramento–San Joaquin Delta region, California, USA. Science of the Total Environment 391:66-75.

DePaolo DJ. 1981. A neodymium and strontium isotopic study of the Mesozoic calc-alkalic granitic batholiths of the Sierra-Nevada and Pennisular Ranges, California. Journal of Geophysical Research 86:10470-10488.

Domagalski J. 2001.Mercury and methylmercury in water and sediment of the Sacramento River Basin, California. Applied Geochemistry 16:1677-1691.

Elrick KA, Horowitz AJ. 1987. Analysis of rocks and sediments for mercury, by wet digestion and flameless cold vapor atomic absorption. U.S. Geological Survey Open-File Report 86-596. 16 p.

Faure G. 1986. Principles of isotope geology, 2nd edition. New York (NY): J. Wiley & Sons. 589 p.

Frost CD, Winston D. 1987. Nd isotope systematics of coarse and fine-grained sediments: examples from the middle Proterozoic Belt-Purcell Supergroup. Journal of Geology 95:309-327.

Fuller CC. 1982. The use of ^{210}Pb, ^{234}Th, and ^{137}Cs as tracers of sedimentary processes in San Francisco Bay, California [Master's thesis]. Available from: University of Southern California. 215 p.

Fuller CC, van Geen A, Baskaran M, Anima R. 1999. Sediment chronology in San Francisco Bay, California defined by ^{210}Pb, ^{234}Th, ^{137}Cs, and ^{239,240}Pu. Marine Chemistry 64:7-27.

Gilbert GK. 1917. Hydraulic-mining debris in the Sierra Nevada. U.S. Geological Survey Professional Paper 105. 154 p.

Goldstein SL, O'Nions RK, Hamilton PJ. 1984. A Sm-Nd isotopic study of atmospheric dusts and particulates from major river systems. Earth and Planetary Science Letters 70:221-236.

Heim WA, Coale KH, Stephenson M, Choe K-Y, Gill GA, Foe C. 2007. Spatial and habitat based variations in total and methyl mercury concentrations in surficial sediments in the San Francisco Bay-Delta. Environmental Science and Technology 41:3501-3507.

Heinz GH, Hoffman DJ. 1998. Methylmercury chloride and selenomethionine interactions on health and reproduction in mallards. Environmental Toxicology and Chemistry 17:139–145.

Higgins SA, Jaffe BE, Fuller CC. 2007. Reconstructing sediment age profiles from historical bathymetry changes in San Pablo Bay, California. Estuarine and Coastal Shelf Science 73:165-174.

Higgins SA, Jaffe BE, Smith RE. 2005. Bathychronology: reconstructing historical sedimentation from bathymetric data in GIS. U.S. Geological Survey Open-File Report OFR-2005-1284. 19 p.

Hornberger MI, Luoma SN, van Geen A, Fuller CC, Anima R. 1999. Historical trends of metals in the sediments of San Francisco Bay, California. Marine Chemistry 64:39-55.

Hunerlach MP, Rytuba JJ, and Alpers CN. 1999 Mercury contamination from hydraulic placer-gold mining in the Dutch Flat mining district, California. In: Morganwalp, DW, Buxton, HT, editors. U.S. Geological Survey Toxic Substances Hydrology Program-Proceedings of the Technical Meeting; 1999, Mar 8-12; Charleston, South Carolina. Volume 2 of 3: Contamination of hydrologic systems and related ecosystems. U.S. Geological Survey Water-Resources Investigations Report 99-4018B. p 179-189.

Ingram BL, Ingle JC, Conrad ME. 1996. A 2000-yr record of Sacramento-San Joaquin river inflow to san Francisco Bay estuary, California. Geology 24:331-334.

Ingram BL, Sloan D. 1992. Strontium isotopic compositions of estuarine sediments as paleosalinity-paleoclimate indictors. Science 255:68-72.

Jacobson M, Kratochvil A. 1998. Can an impoverished country in South America survive a gold-mining boom? Natural History 107(7):47-59.

Jaffe BE, Smith RE, and Torresan LZ. 1998. Sedimentation and bathymetric change in San Pablo Bay: 1856-1983: U.S. Geological Survey Open-File Report 98-759.

James LA. 1989. Sustained storage and transport of hydraulic mining sediment in the Bear River, California. Annals Association of American Geographers 79:570-592.

James LA. 1991a. Quartz concentration as an index of sediment mixing: hydraulic mine-tailings in the Sierra-Nevada, California. Geomorphology 4:125-144.

James LA. 1991b. Incision and morphologic evolution of an alluvial channel recovering from hydraulic mining. Geological Society of America Bulletin 103:723-736.

James LA. 2005. Sediment from hydraulic mining detained by Englebright and small dams in the Yuba basin. Geomorphology 71:202-206.

Krauskopf KB. 1967. Introduction to geochemistry. New York (NY): McGraw-Hill. 721 p.

Lindgren W. 1911. The Tertiary gravels of the Sierra Nevada of California. U.S. Geological Survey Professional Paper 73. 226 p.

Linn AM, DePaolo DJ, Ingersoll RV. 1992. Nd-Sr isotopic, geochemical, and petrographic stratigraphy and paleotectonic analysis: Mesozoic Great Valley forearc sedimentary rocks of California. Geological Society of America Bulletin 104:1264-1279.

Luoma SN, Rainbow PS. 2008. Metal contamination in aquatic environments: science and lateral management. Cambridge (UK): Cambridge University Press. 588 p.

Malm O. 1998. Gold mining as a source of mercury exposure in the Brazilian Amazon. Environmental Research 77A:73-78.

Marvin-DiPasquale MC, Agee JL, Bouse RM, Jaffe BE. 2003. Microbial cycling of mercury in contaminated pelagic and wetland sediments of San Pablo Bay, California. Environmental Geology 43:260–267.

Marvin-DiPasquale MC, Agee JL, McGowan C, Oremland RS, Thomas M, Krabbenhoft D, Gilmour CC. 2000. Methyl-mercury degradation pathways: a comparison among three mercury-impacted ecosystems. Environmental Science and Technololgy 34:4908-4916.

McLennan SM, McCulloch MT, Taylor SR, Maynard JB. 1989. Effects of sedimentary sorting on neodymium isotopes in deep-sea turbidites. Nature 337:547-549.

Meech JA, Veiga MM, Tromans D. 1998. Reactivity of mercury from gold mining activities in darkwater ecosystems. Ambio 27:92-98.

Mergler D, Bélanger S, Larribe F, Panisset M, Bowler R, Baldwin M, Lebel J, Hudnell K. 1998. Preliminary evidence of neurotoxicity associated with eating fish from the Upper St. Lawrence River Lakes. Neurotoxicology 4-5:691-702.

Morel FMM, Kraepiel AM, Amyot M. 1998. The chemical cycle and bioaccumulation of mercury. Annual Review of Ecology and Systematics 29:543-566.

Nesbitt HW, Young GM. 1982. Early Proterozoic climates and plate motions inferred from major element of lutites. Nature 299:715-717.

Nichols FH, Cloern JE, Luoma SN, Peterson DH. 1986. The modification of an estuary. Science 231:567-573.

Nriagu JO. 1994. Mercury pollution from the past mining of gold and silver in the Americas. Science of the Total Environment 149:167-181.

Peterson DH, Noble M, Smith RE. 1993. Suspended sediment in San Francisco Bay estuary, California – recent history and available data sets. Water Resources Investigations Report 93-4128. Sacramento (CA): U.S. Geological Survey. 35 p.

Ritson PI, Bouse RM, Flegal AR, Luoma SN. 1999. STable lead isotopic analyses of historic and contemporary lead contamination of San Francisco Bay estuary. Marine Chemistry 64:71-83.

Schallowitz AL. 1964. Shore and sea boundaries. U.S. Coast and Geodectic Survey Publication 10-1(2). 749 p.

Schoellhamer DH. 2009. Suspended sediment in the Bay: past a tipping point. In: The pulse of the estuary. Monitoring and managing water quality in the San Francisco Bay Estuary. SFEI Contribution 583. Oakland (CA): SFEI. p 56-66.

Schweickert RA. 1981. Tectonic evolution of the Sierra Nevada range. In: Ernst WG, editor. The geotectonic development of California. Englewood Cliffs (NJ): Prentice-Hall. p 87-131.

Steding DJ, Dunlap CE, Flegal AR. 2000. New isotopic evidence for chronic lead contamination in the San Francisco Bay estuary system: implications for the persistence of past industrial lead emissions in the biosphere. Proceedings of the National Academies of Science 97(21):11181-11186.

Taylor SR, McLennan SM. 1985. The continental crust: its composition and evolution. Oxford (UK): Blackwell Scientific Publications. 312 p.

van Geen A, Luoma SN. 1999. The impact of human activities on sediments of San Francisco Bay, California: an overview. Marine Chemistry 64:1-6.

van Geen A, Valette-Silver NJ, Luoma SN, Fuller CC, Baskaran M, Tera F, Klein J. 1999. Constraints on the sedimentation history of San Francisco Bay from ^{14}C and ^{10}Be. Marine Chemistry 64:29-38.

Wiener JG, Bodaly RA, Brown SS, Lucotte M, Newman MC, Porcella DB, Reash RJ, Swain EB. 2007. Monitoring and evaluating trends in methylmercury accumulation in aquatic biota. In: Harris R, Krabbenhoft DP, Mason R, Murray MW, Reash R, Saltman T, editors. Ecosystem responses to mercury contamination: indicators of change. Pensacola (FL): SETAC Press. p 87-122.

Yeend WE. 1974. Gold-bearing gravel of the ancestral Yuba River, Sierra Nevada, California. U.S. Geological Survey Professional Paper 772. 44 p.